Titre: Title:	Electrospun Cellulose Acetate and Metal Oxide Composite Membranes for Water Filtration Applications
Auteur: Author:	Caitlin Kennedy-Hoyland
Date:	2021
Type:	Mémoire ou thèse / Dissertation or Thesis
Référence: Citation:	Kennedy-Hoyland, C. (2021). Electrospun Cellulose Acetate and Metal Oxide Composite Membranes for Water Filtration Applications [Master's thesis, Polytechnique Montréal]. PolyPublie. https://publications.polymtl.ca/9986/

URL de PolyPublie: PolyPublie URL:	https://publications.polymtl.ca/9986/
Directeurs de recherche: Advisors:	Abdellah Ajji, & Marie-Claude Heuzey
Programme: Program:	Génie chimique

POLYTECHNIQUE MONTRÉAL

affiliée à l'Université de Montréal

Electrospun Cellulose Acetate and Metal Oxide Composite Membranes for Water Filtration Applications

CAITLIN KENNEDY-HOYLAND

Département de génie chimique

Mémoire présenté en vue de l'obtention du diplôme de *Maitrise ès sciences appliquées*

Génie chimique

Décembre 2021

POLYTECHNIQUE MONTRÉAL

affiliée à l'Université de Montréal

Ce mémoire intitulé :

Electrospun Cellulose Acetate and Metal Oxide Composite Membranes for Water Filtration Applications

présenté par **Caitlin KENNEDY-HOYLAND**

en vue de l'obtention du diplôme de *Maîtrise ès sciences appliquées*

a été dûment accepté par le jury d'examen constitué de :

Dominique CLAVEAU-MALLET, présidente
Abdellah AJJI, membre et directeur de recherche
Marie-Claude HEUZEY, membre et codirectrice de recherche
Nathalie TUFENKJI, membre externe

RÉSUMÉ

Des membranes en acétate de cellulose ont été testées pour leur capacité à éliminer les microplastiques, l'arsenic (V) et le cuivre (II) de l'eau par filtration directe. À cette fin, sept membranes composites en acétate de cellulose (CA) et en oxyde métallique ont été préparées par électrofilage en solution pour des applications de filtration. Les membranes préparées avaient des diamètres de fibres allant de 0,4 à 0,9 µm avec des tailles de pores moyennes variant de 2 à 7 µm. Toutes les membranes ont réussi à éliminer les particules de plastique d'un diamètre supérieur à 15-20 µm. Les différentes compositions de membranes ont eu un succès variable dans l'élimination de l'arsenic, la membrane noyée dans l'oxyde de fer à 2,5 % ayant obtenu un rejet de 70 % de l'arsenic, tandis que le taux d'élimination le plus faible (0 %) a été obtenu par la membrane composite d'oxyde de fer à 0,5 %. Les résultats de l'élimination de l'ion cuivre (II) de l'eau n'étaient pas concluants, mais les tendances générales des données montrent que les membranes étaient surtout inefficaces pour éliminer le cuivre à des concentrations d'environ 0,5 g/L et à un pH de 4. Cependant, l'élimination du cuivre pour toutes les membranes approchait 80 % à des niveaux de pH neutres, le cuivre étant alors principalement dans un état solide oxydé, ce qui est prometteur pour l'élimination des particules. Ceci a été interprété comme un succès relatif dans les capacités de filtration par rapport aux travaux précédents sur des membranes similaires. L'ajout d'oxydes métalliques n'a pas montré une amélioration suffisamment significative de la qualité de la membrane pour recommander l'utilisation de membranes composites par rapport aux tapis de CA purs.

ABSTRACT

Cellulose acetate membranes were tested for their ability to remove microplastics, arsenic (V), and copper (II) from water via direct filtration. For this purpose, seven cellulose acetate (CA) and metal oxide composite membranes were prepared by solution electrospinning for filtration applications. The prepared membranes had fiber diameters ranging from 0.4 to 0.9 μm with the average pore sizes of the membranes varying from 2 to 7 μm. All membranes were successful in removing plastic particles above 15-20 μm in diameter. The different membrane compositions had varying success at arsenic removal with the 2.5% iron oxide embedded membrane achieving 70% arsenic rejection while the lowest removal rate of 0% was achieved by the 0.5% iron oxide composite membrane. The results of copper (II) ion removal from water were inconclusive, however the general trends of the data shows that the membranes were mostly ineffective at removing copper at concentrations around 0.5 g/L and a pH of 4. However, copper removal for all membranes approached 80% at neutral pH levels, at which point the copper was predominantly as a solid oxidized state. This was interpreted as a relative success in filtration capabilities compared to previous works on similar membranes. The addition of metal oxides did not show a significant enough improvement in membrane quality to recommend the use of composite membranes over neat CA mats.

TABLE OF CONTENTS

LIST OF TABLES

LIST OF FIGURES

LIST OF SYMBOLS AND ABBREVIATIONS

Ac	Acetone
CA	Cellulose Acetate
DMAc	N,N-Dimethylacetamide
ICP-MS	Inductively Coupled Plasma Mass Spectrometry
I.O.	Iron Oxide
LDPE	Low density polyethylene
MNP	Micro and nanoplastics
MP	Microplastics
NP	Nanoparticles
PVC	Polyvinyl chloride
PEX	Cross-linked polyethylene
POU	Point of Use
PS	Polystyrene
SEM	Scanning electron microscope
WHO	World Health Organization
wt%	Weight percent

LIST OF APPENDICES

CHAPTER 1 INTRODUCTION

1.1 Context

Contaminated drinking water threatens populations worldwide. From a lack of proper water treatment facilities in developing communities [1], to incidents affecting tap water in regions of first-world nations (e.g. Flint, MI, USA) [2], point of use (POU) filtration is a common method used to mitigate the risks of contaminated water. POU filtration is the treatment of water at the point of consumption, such as at home, in schools, at work, etc… There are many different POU filtration systems, both in terms of set up and targeted contaminants, some examples include membranes, ceramic filters, and activated carbon [1], [2]. Common drinking water pollutants include microbes, sediment, persistent organic pollutants, and heavy metals [1]. Micro and nanoplastics (MNP) pollution in fresh water systems is an example of a pollutant of emerging concern [3], [4].

In the United States, the need for residential water treatment devices is spurred by lack of process control or regulations, contamination of the feed waters by industrial interference (e.g. fracking) [5] or existing infrastructure (e.g. lead and plastic pipes), or random incidents at treatment plants, and so many households have turned to residential water treatment to reduce their risk of contamination [2]. A literature review of multiple point of use filtration systems in the US conducted by Brown et al. [2] showed that the use of these systems proved effective at reducing inorganic and organic chemical contaminants in drinking water, however the removal success varied significantly between regions and targeted pollutants.

Heavy metal pollution can also be found in certain regions of Quebec above recommended safety levels. Examples of the need for POU filtration include lead contamination in Montreal by old pipe systems [6] and arsenic contamination of some well water systems [7]. Recent studies have also observed the presence of plastic particles in tap water worldwide [8].

1.2 Paper objectives and organization

The scope of this project encompasses the fabrication of electrospun membranes from lab grade materials as well as the testing of these membranes for their filtration capabilities of selected pollutants. The objective of this research is to create a water filtration membrane by solution

electrospinning. A fibrous cellulose acetate membrane with embedded metal oxide nanoparticles will be used to remove arsenic and microplastics by filtration. This work is quite novel since microplastics is a relatively new field of investigation in terms of assessment and removal, and few works deal with arsenic and/or microplastic removal by cellulose acetate membranes. The produced membranes morphologies and porosities were investigated by scanning electron microscope (SEM) imagery and pycnometer based porosity measurements, respectively. Filtration capabilities of the membranes were evaluated by comparison of the feed and filtrate solution compositions. Inductively coupled plasma mass spectrometry (ICP-MS) was used for the measurement of arsenic concentrations in solution and microscopy was used to evaluate plastic particle size distributions in suspensions.

The organization of this paper is as follows: A literature review is presented in the subsection below to provide a context on topics addressed later on and to show the latest research developments in the area of interest. Chapter 3 holds most of the experimental methods and data for this study in the form of an article for publication. This includes membrane morphology after electrospinning, and arsenic and polystyrene filtration capabilities of the membranes. Supplementary experimental results can be found in Chapter 4, which gives a more in depth description of the electrospinning optimization process as well as showing some complementary results for membrane filtration. This chapter also relates these findings to the context of the article. Chapter 5 contains a general discussion of all presented results. Finally, Chapter 6 lists general conclusions of this paper and provides recommendations for future work.

CHAPTER 2 LITERATURE REVIEW

2.1 Pollutants

Arsenic is a chemical found throughout the earth in both organic and inorganic forms. The organic forms are less toxic and commonly contaminates communities through food sources such as seafood, while the inorganic forms are mostly hazardous by water contamination with several countries' groundwater sources exceeding toxic values. The chemical is a known carcinogen and long term exposure to levels above the WHO recommended limit of 10 μg/L in drinking water is linked to several health issues including cardiovascular disease, and diabetes [9]. Arsenic pollution sources in water include natural ores located in groundwater, and contamination by industrial processes. Mining is the primary source of this pollution; however many other industries can contribute to contamination including pesticide use, tanning, and wood treatment [10].

There are many other metal ions which can be harmful to public or environmental health above certain concentrations. One example is copper ions, which can lead to weakness at high exposure levels. Copper (II) ions are a useful chemical to test metal ion removal as they have a blue colour in solution which aids in observing removal effectiveness [11].

Another water pollutant of emerging concern is microplastics. Microplastics have been more commonly observed in ocean waters, possibly because of a lack of investigation into plastic pollution in freshwater and wastewater systems until recently, however significant concentrations of micro and nanoplastics (MNPs) have been found in various lakes and rivers [3], as well as drinking water [8], worldwide. One study found areas of microplastics concentrations in the St Lawrence river (Quebec, Canada) which were comparable to the highest density of MNP pollution in marine environments [4]. They also found evidence that MNPs may be transported to lake systems by river currents, meaning this problem most likely does not remain localized to the pollution source. Microplastics encompass all plastic types and particle shapes below ~5 mm in diameter [3]. While there is no standard microplastics lower size limit, generally plastic particles below 0.2 mm are considered nanoplastics (or below ~100 nm if using a general nanomaterial definition) [3]. These pollutants can be caused by primary sources, including use of MNPs in final products, such as facial cleansers, or can be a result of waste by specialized processes found in the auto or medical industries. Secondary MNP sources are caused by chemical or physical degradation

of larger plastic waste in the environment (such as in the "Great Pacific Garbage Patch" [12]) or in wastewater (e.g. by washing plastic fabrics) [3]. MNPs have become a more common concern in research in recent years with increased plastic pollution, improved detection technologies, and environmental research focuses. The exact nature of the impacts of MNPs in freshwater systems is still being investigated, however it is known that these products can lead to physical harm or even death when aquatic organisms mistake them for food [3]. MNPs may also provide surface which allow for the adsorption of persistent organic pollutants (POPs) onto the surface, which can be desorbed back into the water system at a new location, or bioaccumulation of the pollutants up the food chain from ingestion by small organisms [3]. The leaching of plasticizers (a POP) from microplastics can damage water health and lead to further degradation of the plastic particles by increasing brittleness. One study on microplastics produced from teabags showed a negative impact on *D. Magma* (water flea) health from existing in MNP polluted solutions, ingestion of the MNPs by the animals was evident. These effects were more obvious with MNPs thought to have absorbed metals such as arsenic from the tea [13]. They are also believed to pose a risk to the ecosystem by certain MNPs providing ideal host sites for harmful microbial or viral growth. While MNPs are still a developing field of research for both analysis and removal, the current evidence suggests it's an important field to investigate for environmental and public health [3].

2.2 Membrane filtration

The standard water treatment technologies used for public water systems are coagulation and flocculation and settling, filtration by a variety of media, and disinfection. An example of a water treatment plant is shown in Figure 2.1.

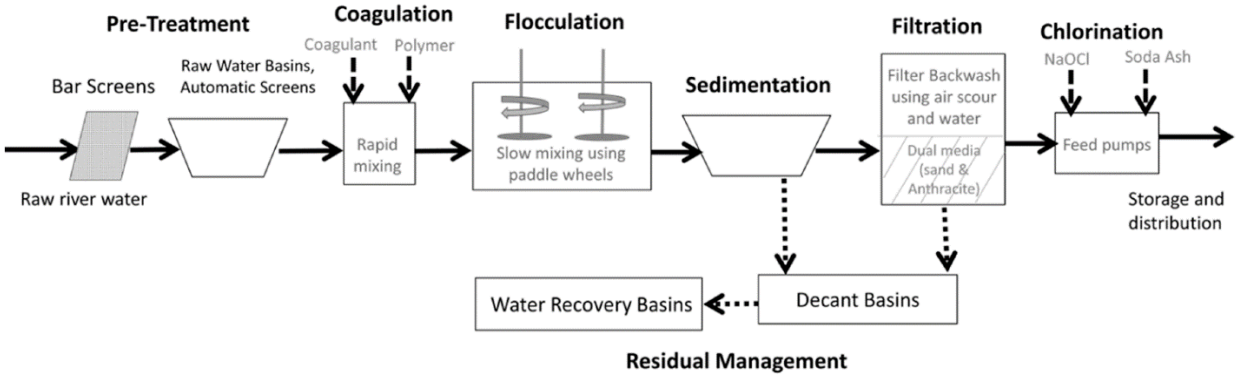

Figure 2.1 Example of a public water treatment system [14]

Other methods of water treatment for drinking water include chemical treatment, boiling, adsorption, oxidation, and more. Membrane filtration is a water treatment technology which has evolved over the late twentieth century. Newly developed technologies can provide more sustainable and efficient removal of contaminants compared to standard treatment [15]. Nanofiltration membranes have shown success in the treatment of both groundwater and surface water, targeting the full array of water pollutants [16]. The use of membrane filtration in water filtration has some disadvantages however, such as membrane tearing and fouling. There are several types of membrane fouling, such as scaling, biofouling, and colloidal fouling. Fouling severity is determined by the feed water composition, membrane surface properties, and flux properties, considering the effects of fouling before membrane creation can help mitigate its effects and extend the lifetime of a membrane [16].

There are four main types of membrane filtration (plus particulate filtration). They are differentiated by their pore size and targeted pollutants for removal by membrane filtration. These membrane types are summarised in Table 2.1.

Table 2.1 Membrane filtration types [17], [18]

Filtration type	**Pore Size (µm)**	**Targeted Pollutants**
Reverse Osmosis	<0.001	Ions
Nanofiltration	0.001-0.01	Ions, Low molecular weight compounds
Ultrafiltration	0.01-0.1	Viruses, Proteins, Large organic compounds
Microfiltration	0.1-1	Microbes, Colloids, Turbidity, Smaller suspended particles
Particulate Filtration	>1	Visible suspended particles

The removal of microplastics is done with microfiltration or particulate filtration membranes, this removal mechanism is largely size based exclusion due to the microplastics being of a larger size than the membrane pores. Ion removal mechanisms can be employed in a microfiltration membrane, while not technically being classified as nanofiltration or ultrafiltration the microfiltration membranes can still work to remove arsenic ions.

There are two main separation mechanisms for ion removal, separation by size exclusion and rejection by surface charge. Size exclusion of membranes is the failure of particles above a certain size to pass through the membrane because they are too large to make their way through the pore network. Membrane surface charge helps in the removal of certain contaminants, in some cases

there are ionic interactions between ionizable surface groups and pollutants which can lead to adsorption of the particles onto the surface. The surface polarity can also lead to electrostatic repulsion of similarly charged particles in nanoscale pores, rejecting pollutants while allowing water to pass through. The polarity of the surface groups can be altered with different permeate pH values for chemical species with isoelectric points [16].

Characteristics of membranes which are important for filtration include chemical and thermal stability, porosity and pore size, mechanical durability, and surface charge [15]. The stability of the membrane can prevent deterioration, and hydrophilic materials help to reduce fouling, both of these properties improve the membrane's lifetime. Porosity, pore size, and surface charge determine the membrane's ability to reject a given pollutant, and improved mechanical properties help to prevent tearing and allow for higher permeate flux [15].

2.3 Electrospinning

Electrospinning is a method of producing polymer fibers which has been around since the first patents defining the concept were filed in 1902 [19]. This method of producing ultrafine polymer fibers involves extruding a polymer solution (or liquid polymer in melt spinning) via a syringe pump where it passes through a spinneret (often a blunt tipped needle) and is deposited onto a collector. A high voltage power supply is used to create a differential between the spinneret and the collector, this allows for electrostatic forces to draw the polymer into fine fibers. The basic electrospinning setup is shown in Figure 2.2.

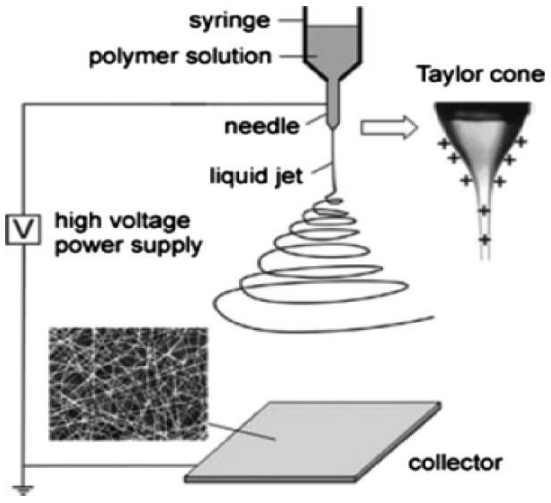

Figure 2.2 Basic solution electrospinning setup using a plaque collector [20]

The charged polymer solution first forms a Taylor cone on the spinneret tip, caused by surface tension and electrostatic forces on an extruded droplet, from this cone, a jet of polymer solution is ejected, travelling towards the oppositely charged collector plate along the path of the imposed electric field. The jet begins in a straight line and as the jet is elongated, bending instabilities caused it to spiral with increasing radius towards the collector. The stretched jet eventually solidifies on the path to the collector (due to solvent evaporation in solution spinning) where it is deposited, usually in a nonwoven, randomly oriented fiber mat. Other instabilities, such as branching and capillary, caused by a variety of experimental and environmental factors can cause beaded and/or irregular fibers. Electrospun mats can be differently oriented, and fibers can be tailored to have different fiber and/or surface morphologies by using variations of the traditional electrospinning setup [19].

Electrospinning can be done both at a laboratory and an industrial scale. Scaling up of the electrospinning process can be difficult due to the need for reproducibility of the precise electrospun fiber morphologies, yet there are many commercial products that use electrospinning as a production method [21]. Some of these commercial products include face masks, air filters, and textiles. This method of production can also be seen in more specific applications in the biomedical industry such as cell culture scaffolds, dialysis membranes, and covered stents [22]. Up-scaling of the electrospinning process can be done using a multi-spinneret setup, or more novel processes such as centrifugal electrospinning, and requires strict control of the ambient conditions such as temperature and humidity [21].

2.4 Membrane production

2.4.1 Electrospinning membranes

There are many options for materials when it comes to electrospinning, for solution spinning it is common to use organic polymers in a solvent. Critical factors which determine spinnability include polymer molecular weight and its solubility in a suitable solvent. The solvent choice affects solution surface tension, conductivity, and viscosity, which in turn greatly influences the nature and or presence of resultant fibers. Some spinnable polymers include both natural and synthetic polymers such as polyvinyl chloride, polylactic acid, polystyrene (PS), and chitosan [19]. Composite fibers can also be created with the incorporation of additives, such as nanoparticles, in

the spinning solution. Heat treatment of membranes can be used to weld the spun fibers together at nexus points, which can affect properties such as mat porosity, tensile strength, and chemical and physical stability [19]. Heat treatment can be done by ambient temperature changes, perimeter heating, and hot pressing [23]. There are many applications for electrospun mats, from wound dressing to ‘smart’ materials, to water purification. Electrospinning is highly desirable for water filtration applications as it produces high porosity mats for use in high flux filtration. This method allows for reasonable control over fiber diameter and therefore pore size and distribution and provides extremely high available surface areas. Electrospinning is also a relatively cheap production method for polymer membranes [19]. This experiment will focus on point of use filtration applications, as it focusses on rejecting pollutants in drinking water and will be tested at a low flow rate.

2.4.2 Metal oxides

Additives incorporated into electrospun mats can increase filtration efficiency or widen membrane applications. In the removal of heavy metals from water, metal oxides have been shown to be effective adsorbent materials. Metal oxides likely experience electrostatic interactions with charged metal ions as the primary drive for the adsorption mechanism. The adsorbent materials charge, and therefore their ability to interact with a given pollutant is highly dependent on pH, an example is iron oxide. The surface may have more net positively charged groups in acidic solutions (such as $FeOH^{+}$) or more net negative or neutral groups in basic solutions (such as FeO^{-}). The Eh-pH diagram in Figure 2.3 shows the effect of pH on the surface charge of iron oxide in aqueous media.

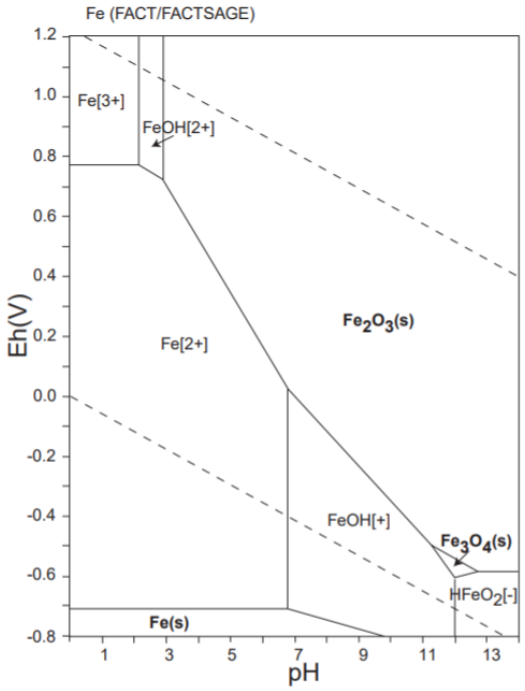

Figure 2.3 Eh-pH diagram of iron oxide

The overall surface charge of metal oxide particles allows for electrostatic attraction or repulsion of heavy metal ions. Previous works have seen success with iron oxide based materials for both As (III) and As (V) adsorbents in neutral solutions [24]. It has also been found that metal oxides, such as ZnO, can affect the membrane surface charge and hydrophilicity which affects arsenic rejection in filtration [25].

2.4.3 Polymer selection

Many polymers were considered for the production of the electrospun filtration membranes. Options were compared based on how their properties related to water filtration applications as well as their electrospinnability. Table 2.2 summarises a few of the considered polymers and relevant properties.

Table 2.2 Summary of polymer options and properties

Polymer	**Water soluble?**	**Electrospun fiber diameter [µm]**	**E [MPa]**	**Biobased/ Biodegradable [26]**
Cellulose Acetate [27]	No	0.08-58	10	Both

Polylactic acid [28], [29]	No	1	10	Both
Chitosan [30], [31]	Conditionally	N/A	7	Both
Polyvinyl chloride [32], [33]	No	0.3	12	Neither
Polyethylene oxide [34]	Yes	N/A	N/A	Biodegradable
PMMA [32]	No	0.5	13	Neither

Table 2.2 shows that cellulose acetate meets all the desirable criteria for the chosen application, with previously electrospun fiber diameters reaching a low of around 80 nm, reasonable mechanical properties, and insolubility in water it is useful for the creation of a water filtration membrane. CA was chosen over other suitable polymers, such as PVC, due to its sustainability. The use of a biopolymer was desired to minimize the overall environmental impact of the project. Cellulose acetate was also chosen because of its success in previous works for incorporated metal oxide nanoparticles into electrospun fibers. There is a gap in the literature concerning CA water filtration membranes for the removal of the target pollutants.

2.4.4 Cellulose acetate

Cellulose acetate (CA) is a very useful polymer for water filtration processes, having reasonable mechanical properties and thermal resistance [35]. Some of the advantages of using CA is its low cost, sustainability (being both biobased and conditionally biodegradable) [36], and easy processing. Cellulose acetate polymer has ester (slightly polar) and hydroxyl (polar) functional groups available on the surface as shown by Figure 2.4.

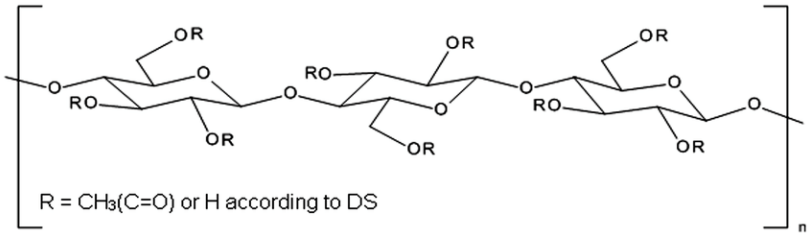

Figure 2.4 Basic chemical structure of cellulose acetate polymer (where DS=degree of substitution of acetylation) [37]

The degree of acetylation effects the polymer's polarity and hydrophilicity, as it creates a higher ratio of the less polar acetyl groups. In the field of water filtration, CA is useful due to its

hydrophilic nature [35], hydrophilic membranes are less at risk for biofouling, enhance rejection of certain pollutants, and encourage a high water flux [16].

Cellulose acetate was first discovered in 1865 by the acetylation of cellulose, and from 1903-1905 work was done to produce the acetone soluble cellulose diacetate by hydrolysis of fully acetylated cellulose. Cellulose acetate has had applications throughout the years including coatings on aircraft wings, textiles, cigarette filters, photo film, safety goggles and more. Although the development of new polymer materials has led to a reduction in cellulose acetate popularity in certain industries, the polymer is still useful in films, membranes, and injection molded parts [38].

Cellulose is treated with both acetic acid, and acetic anhydride with the aid of a catalyst to produce cellulose triacetate. Hydrolysis of the cellulose triacetate to produce cellulose diacetate can be done by treating the polymer with water [38]. More sustainable methods of CA production have also been investigated which reduce the energy consumption and use of chemical agents in cellulose extraction and acetylation. One example is the production of CA from corncobs by hydrothermal and dilute base treatments, followed by iodine catalyzed acetylation [39].

2.5 Electrospinning CA

Electrospinning of cellulose acetate can be done using a variety of solvent systems. Figure 2.5 shows an example of the achieved morphology of the CA fibers by electrospinning using various solvent systems from the work of Majumder et al. [40].

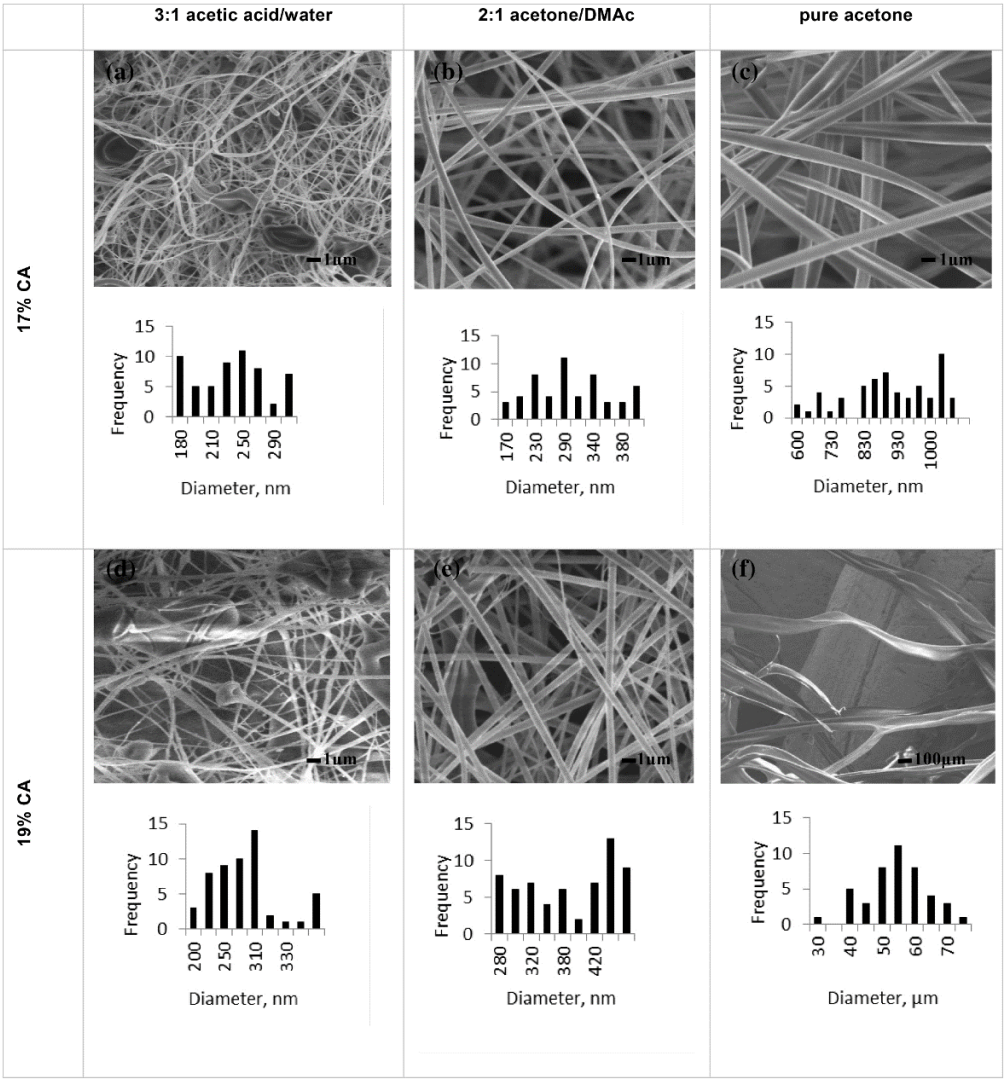

Figure 2.5 Cellulose acetate electrospinning results using varying solution compositions [40]

As shown in Figure 2.5, CA is able to achieve smooth cylindrical fibers in a randomly oriented mat by electrospinning using a binary solvent system of N,N-dimethyl acetamide (DMAc) and acetone. The solution system must have a high enough polymer concentration to allow for chain entanglement, which allows for the stretching of beads into smooth fibers. Beads can also appear when the surface tension of the solution in the needle tip is not balanced by the electrostatic forces, this is seen in a) and d) where the acetic acid/water solution has an insufficient dispersion force. In cases of too high solvent volatility, such as with a pure acetone system, needle clogging is a persistent problem during spinning. The acetone solvent system as seen in c) in Figure 2.5, also causes solvent evaporation before proper fiber elongation, causing large diameter fibers which collapse into ribbon like morphologies, and fiber splitting at the tip. Finally, looking at images b)

and e) one can see the importance of solution viscosity on fiber diameters, the 2:1 Ac:DMAc system produced a stable jet at the needle tip, however increasing polymer concentration increased solution viscosity, producing thicker fibers as a result [40].

2.6 Related works

Previous works which have electrospun cellulose acetate and composite metal oxide/cellulose acetate fibers for various applications appears in Table 2.3 as a non-comprehensive summary.

Table 2.3 Electrospinning cellulose acetate literature summary

Work	**Solid materials**	**Solution composition**	**Average fiber diameter (μm)**	**Proposed application**
Abbasi, et al. 2021 [41]	CA	12 wt% in Acetone (Ac) :Acetic Acid (AA) (1 :2)	15	Component of antibacterial films
Mehdi et al., 2021 [42]	CA	17 wt% in Ac :Dimethyl formamide (DMF) (2:1)	0.3	Antibacterial mats (incorporation of sericin-Ag NPs)
Santos-Sauceda et al., 2021 [43]	CA	11 wt% in 80 Ac:water (80:20)	1.22	Dye decolorization
Ali et al., 2019 [44]	CA	9 wt% in Ac:water (90:10)	1.69	N/A
Omollo et al., 2014 [45]	CA	15 wt% in trifluoroacetic acid	~0.12	High efficiency water filtration -NaCl rejection tested (in between 2 nonwoven polypropylene layers)
Naragund and Panda, 2020 [35]	CA	7-15 w/v% in Methyl ethyl ketone (MEK): N,N-Dimethylacetamide (DMAc) (2:1)	0.08 to 0.24	Membrane for water flux (related properties evaluated)
		11-15 w/v % in MEK:DMAc (1:1)	0.12 to 0.2	
		17-19 % w/v in MEK:DMAc (1:2)	0.12 to 0.16	
Angel et al., 2020 [46]	CA	9 to 15% w/v in acetone	0.4 to 1.3	N/A

Zhou et al., 2016 [47]	CA	12 wt% in DMF:Ac (99 :1)	0.96	High Flux water filtration (MP removal see Table 2.4)
		14 wt% in DMF:Ac (99 :1)	1.30	
		16 wt% in DMF:Ac(99 :1)	1.57	
Majumbder et al., 2019 [40]	CA	17 wt% in Ac :DMAc (2 :1)	0.30	N/A
		19 wt% in Ac :DMAc (2 :1)	0.37	
		17 wt% in Ac	1.0	
		19 wt% in Ac	58	
Ertas and Uyar, 2017 [48]	CA	10% (w/v) in DCM :Methanol (4 :1)	0.62	Water treatment (CA and CA/polybenzoxazine membranes)
		12% (w/v) in DCM :Methanol (4 :1)	0.72	
Han et al., 2008 [49]	CA	17 wt% in AA:water (70:30 to 95:5 (w:w))	~0.2 to 1.3	N/A
Tian et al., 2011 [11]	CA	Ac:DMAc	0.75	Heavy metal adsorption (by PMMA surface modification)
Wang et al., 2016 [50]	CA	Ac:AA (2:1)	2.0	Dye adsorption (silver NP additive)
		Ac:DCM (2:1)	4.6	
		Ac:DCM (1:2)	4.9	
Anitha et al., 2013 [51]	CA	14 wt% in DMF:Ac (4:1)	0.17	Bactericidal, optical, and hydrophobic property investigation
Hassan et al., 2017 [52]	CA	Ac:DMF-varying ratios	0.06-0.15	Phenol decontamination
		Ac:DMAc (2:1)	0.06	
		Ac:DMAc (2:1)	0.15	
	CA-ZnO	2:1 Ac:DMAc	~0.6	
Tsioptsias et al., 2010 [53]	CA	20 wt% in Ac:DMAc (2:1)	~0.6	N/A
	CA-Fe2O3		~0.4 (1.4 wt% Fe2O3) ~0.3 (4.5wt% Fe2O3)	
Matos et al., 2018 [27]	CA	12 wt% in Ac:DMAc (2:1 (w:w))	0.299	Magnetic hyperthermia (by Fe3O4 NPs adsorbed onto or embedded in fibers)
	CA	12 wt% in 63:32:5 Ac:DMAc:water	0.272	
	CA-Oleic Acid stabilized Fe3O4 NPs	11 wt% in 63:32:5 Ac:DMAc:water	0.165	

	CA-DMSA stabilized Fe3O4 NPs	10 wt% in 63:32:5 Ac:DMAc:water	0.161	

The review of the research shows that cellulose acetate is most successfully electrospun using a solvent mixture system with acetone, often Ac:DMAc, with polymer concentrations above 10 wt% in solution. The produced fiber diameters from literature range from 80 nm to 58 μm, often in the order of hundreds of nanometers.

Cellulose acetate blends are also commonly electrospun materials such as the electrospun mats produced by Pittarate et al. [54] who added small amounts of polyethylene oxide (PEO) to the CA polymer solution. These fibers used PEO to incorporate ZnO nanoparticles into the solution and achieved average fiber diameters for the different polymer blend ratios from 0.4 to 1.2 μm, and from 0.9 to 1 μm in diameter for the ZnO/polymer composite mats. In another paper by Luo et al. [55], they were able to create extra porous membranes for Cr(VII) removal by spinning a CA/polyethyleneimine blend and achieved an average fiber diameter of 4.3 μm.

This literature review served as the basis for selecting the parameters to be tested in the electrospinning optimization part of this report. The solvent system most used in previous works for successful spinning of smooth cylindrical fibers was a binary acetone and N-N, dimethylacetamide solution and so this was chosen for experimental testing. Also observed in the literature review was a minimum cellulose acetate concentration in the electrospinning solution of 10 wt% and so this was the starting concentration for preliminary electrospinning tests, with incremental wt% increases until the desired fiber morphology was achieved. All other spinning conditions were varied within the range of values that saw success in literature to optimize the process.

The incorporation of metal oxide nanoparticles into electrospun fibers is seen to have some effect on fiber diameter due to the increased conductivity and viscosity of the composite solutions. In the work of Matos et al. [27] it reduced fiber diameter, and in Hassan et al. [52] it increased fiber diameter.

The incorporation of metal oxides into cellulose acetate mats or membranes have also been shown to improve the physical properties of the polymer product. Matos et al. observed an improvement

in mechanical properties of electrospun mats when comparing neat CA and magnetite-CA composite mats as seen in Figure 2.6 [27].

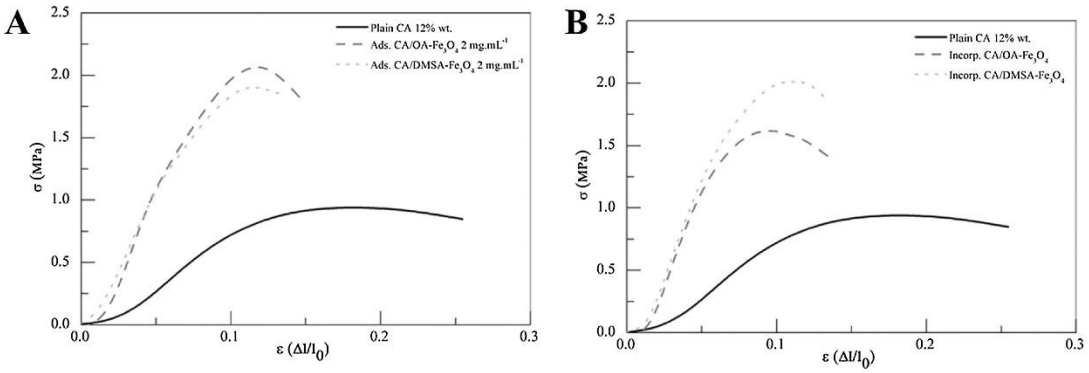

C

Sample	E (MPa)	UTS (MPa)	σ_{EL} (MPa)
Plain CA 12 wt.%	10.2 ± 2.5	0.952 ± 0.063	0.84 ± 0.054
Adsorption CA/OA-Fe_3O_4 0.5 mg.mL^{-1}	40.6 ± 6.7	2.08 ± 0.21	1.29 ± 0.089
Adsorption CA/OA-Fe_3O_4 2 mg.mL^{-1}	35.1 ± 8.7	2.12 ± 0.23	1.28 ± 0.15
Adsorption CA/DMSA-Fe_3O_4 0.5 mg.mL^{-1}	36.0 ± 7.8	1.96 ± 0.16	1.58 ± 0.20
Adsorption CA/DMSA-Fe_3O_4 2 mg.mL^{-1}	29.4 ± 9.9	1.99 ± 0.21	1.66 ± 0.18
Incorporation CA/OA-Fe_3O_4	32.0 ± 4.6	1.64 ± 0.10	1.36 ± 0.090
Incorporation CA/DMSA-Fe_3O_4	33.5 ± 5.6	2.09 ± 0.18	1.49 ± 0.14

Figure 2.6 Mechanical testing results of electrospun CA membranes with magnetite nanoparticles incorporated by surface adsorption and in electrospinning solution [27]

Graph B (which plots stress (σ) against strain (ε)) and the last two lines of table C in Figure 2.6 show the mechanical testing results of CA membranes prepared by the incorporation of surfactant coated iron oxide nanoparticles in the electrospinning solution. Matos et al. found that the incorporation of metal oxide nanoparticles improved Young's modulus (E) of the mats by 3 fold compared to neat CA, the ultimate technical strength (UTS) by 1.7-2 times and increased the elastic limit stretch (σ_{EL}) by around 0.5 to 0.7 MPa.

It is clear from these findings that the incorporating of metal oxide nanoparticles in electrospun cellulose acetate has a positive impact on the product's mechanical properties, it was also found in a study by Abedini et al. [56] that they improve the thermal resistance of the material (see Figure 2.7).

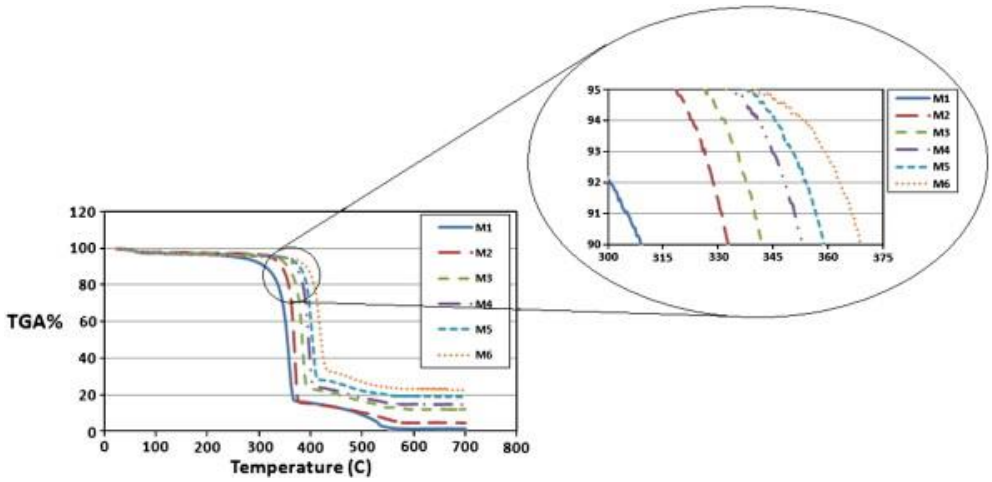

Figure 2.7 Thermogravimetric analysis results of CA and CA-TiO_2 membranes made by phase inversion, where M1 is neat CA and M2 to M6 have TiO_2 contents increasing from 5 to 25% of polymer [56]

As shown by Figure 2.7 the introduction of metal oxide nanoparticles into a CA matrix delays the decomposition of the material due to heating. This was attributed to increased rigidity of the composite compared to neat CA [56].

A summary of the results of previous works concerning arsenic or microplastic removal using cellulose acetate membranes, with or without metal oxide additives are listed in the table below.

Table 2.4 Literature review of relevant cellulose acetate membranes on microplastics removal and arsenic rejection

<table>
<tr><th>Work</th><th>Membrane composition</th><th>Production method</th><th>MP removal</th></tr>
<tr><td>Pizzichetti et al., 2021 [57]</td><td>CA membrane (5µm pore size)</td><td>Commercial product</td><td>Polyamide-20 µm average diameter particles-~100 % mass removed
Polystyrene-75 µm average diameter particles-~94% mass removed</td></tr>
<tr><td>Zhou et al., 2016 [47]</td><td>CA</td><td>Electrospun & hot pressed membrane</td><td>
<table>
<tr><th></th><th colspan="4">Particle size (µm) (Polystyrene)</th></tr>
<tr><th>Fiber diameter (µm)</th><th>5</th><th>2</th><th>0.5</th><th>0.1</th></tr>
<tr><td>0.96</td><td colspan="2" rowspan="3">~100%</td><td>77%</td><td>12%</td></tr>
<tr><td>1.3</td><td>28%</td><td>11%</td></tr>
<tr><td>1.57</td><td>32%</td><td>8%</td></tr>
</table>
</td></tr>
<tr><th>Work</th><th colspan="2">Membrane composition</th><th colspan="2">Production method</th><th>Arsenic rejection</th></tr>
<tr><td></td><td colspan="2">CA</td><td colspan="2"></td><td>~30-40% removal</td></tr>
</table>

Durthi et al., 2018 [25]	Mixed membrane: 94wt% CA, 6% ZnO nanoparticles (diameter 50-500 nm)	Phase inversion- solution cast 100 and 200 μm thickness	~40-60% removal

There are many cellulose acetate membranes produced by a variety of methods which investigated filtration of different pollutants [48] or in different media [58], however there aren't many cellulose acetate membranes in the literature that look at arsenic rejection and/or microplastic removal, as highlighted in Table 2.4. There were also some works in literature which looked at water filtration using cellulose acetate blend membranes, for example the polyphenylsulfone (PPSU)/cellulose acetate membranes created by Kumar et al. in 2020 and 2021. They looked at PPSU/CA hollow fiber membranes with embedded ZrO_2 (2020) and ZnO-MgO (2021) particles and found arsenate rejection rates of 70-87% and ~80% respectively [59], [60].

CHAPTER 3 ARTICLE 1: ELECTROSPUN CELLULOSE ACETATE MEMBRANES WITH EMBEDDED METAL OXIDE NANOPARTICLES FOR MICROPLASTICS AND ARSENIC FILTRATION

This article was authored by Caitlin Kennedy-Hoyland, Marie-Claude Heuzey, and Abdellah Ajji, and was submitted to *Water Research* on Nov. 18, 2021. The paper was under review as of Nov. 28, 2021.

3.1 Abstract

Cellulose acetate membranes were tested for their ability to remove microplastics and arsenic (V) from water via direct filtration. For this purpose, seven cellulose acetate (CA) and metal oxide composite membranes were prepared by solution electrospinning for filtration applications. The prepared membranes had fiber diameters ranging from 0.4 to 0.9 µm with the average pore sizes of the membranes varying from 2 to 7 µm. All membranes were successful in removing plastic particles above 15-20 µm in diameter. The different membrane compositions had varying success at arsenic removal with the 2.5% iron oxide embedded membrane achieving 70% arsenic rejection while the lowest removal rate of 0% was achieved by the 0.5% iron oxide composite membrane. This was interpreted as a relative success in filtration capabilities compared to previous works on similar membranes. The addition of metal oxides did not show a significant improvement in membrane quality to recommend the use of composite membranes over neat CA mats.

3.2 Introduction

Contaminated drinking water threatens populations worldwide. From a lack of proper water treatment facilities in developing communities [1], to incidents affecting tap water in regions of first-world nations (e.g. Flint, MI, USA) [2], point of use (POU) filtration is a common method used to mitigate the risks of contaminated water. POU filtration is the treatment of water at the point of consumption, such as at home, in schools, at work, etc.… There are many different POU filtration systems, both in terms of set up and targeted contaminants, some examples include membranes, ceramic filters, activated carbon, etc.… [1], [2]. Common drinking water pollutants include microbes, sediment, persistent organic pollutants, and heavy metals [1]. While some more novel water pollution contaminants have emerged in recent years, such as micro and nanoplastics

(MNP) pollution in freshwater systems [3], [4]. This study hopes to investigate the use of electrospun membranes for POU filtration with regards to the heavy metal arsenic, and emerging MNP pollutants.

Arsenic is a chemical found throughout the earth in both organic and inorganic forms. The organic form is less toxic and commonly contaminates communities through food sources such as seafood, while the inorganic form is mostly hazardous by water contamination with several countries' groundwater sources exceeding toxic values. The chemical is a known carcinogen and long term exposure to levels above the WHO recommended limit of 10 μg/L is linked to several health issues including cardiovascular disease, and diabetes [9]. Arsenic pollution sources in water include natural ores located in groundwater, and contamination by industrial processes. Mining is the primary source of this pollution; however many other industries can contribute to contamination including pesticide use, tanning, and wood treatment [10].

Another water pollutant of emerging concern is microplastics. Although the problem of MNP is mostly associated with their adverse impacts on aquatic ecosystem, the public is progressively made aware of their presence in tap water [61]. Concentrations of 10^{-2}-10^{8} particles/m^3 have been reported in various studies, however the quality of analytical methods for assessment varies [8]. Plastic is used ubiquitously in water systems [8]. Ultrafiltration membranes, ion exchange resins, PVC (polyvinyl chloride) water mains and PEX (cross-linked polyethylene) residential piping [62] are examples of potential sources of water contamination by MNP. Most faucets also use nowadays connection pipes made of polymers while point-of-use filtration devices (such as pitcher filters) are also fabricated with various polymeric materials. Therefore, it is of interest to develop polymeric membranes for POU applications which not only limit the release of MNP in treated waters but also filter out MNP already present in tap water.

Electrospinning is a method of producing polymer fibers which has been around since the first patents defining the concept were filed in 1902 [19]. This method of producing ultrafine polymer fibers involves extruding a polymer solution (or liquid polymer in melt spinning) via a syringe pump where it passes through a spinneret (often a blunt tipped needle) and is deposited onto a collector. A high voltage power supply is used to create a differential between the spinneret and the collector, this allows for electrostatic forces to draw the polymer into fine fibers. The charged polymer solution first forms a Taylor cone on the spinneret tip, caused by surface tension and

electrostatic forces on an extruded droplet, from this cone, a jet of polymer solution is ejected, travelling towards the oppositely charged collector plate along the path of the imposed electric field. The jet begins in a straight line and as the jet is elongated, bending instabilities caused it to spiral with increasing radius towards the collector. The stretched jet eventually solidifies on the path to the collector (due to solvent evaporation in solution spinning) where it is deposited, usually in a nonwoven, randomly oriented fiber mat. Other instabilities, such as branching and capillary, caused by a variety of experimental and environmental factors can cause beaded and/or irregular fibers. Electrospun mats can be differently oriented, and fibers can be tailored to have different fiber and/or surface morphologies by using variations of the traditional electrospinning setup [19].

There are many options for materials when it comes to electrospinning, for solution spinning it is common to use organic polymers in a solvent. Critical factors which determine spinnability include polymer molecular weight and its solubility in a suitable solvent. The solvent choice affects solution surface tension, conductivity, and viscosity which greatly influences the nature and or presence of resultant fibers. Some spinnable polymers include both natural and synthetic polymers such as PVC, PLA, PS, and chitosan [19]. Composite fibers can also be created with the incorporation of additives, such as nanoparticles in the spinning solution. Heat treatment of membranes can be used to weld the spun fibers together at nexus points, which can affect properties such as mat porosity, tensile strength, and chemical and physical stability [19]. Heat treatment can be done by ambient temperature changes, perimeter heating, and hot pressing [23]. There are many applications for electrospun mats, from wound dressing to ‘smart’ materials to water purification. Electrospinning is highly desirable for water filtration applications as it produces high porosity mats for use in high flux filtration. They allow for reasonable control over fiber diameter and therefore pore size and distribution and provide extremely high available surface areas. Electrospinning is also a relatively cheap production method for polymer membranes [19]. This experiment will focus on point of use filtration applications, as it focussed on rejecting selected pollutants and will be tested at a low flow rate.

Additives incorporated into electrospun mats can increase filtration efficiency or widen membrane applications. In the removal of heavy metals from water, metal oxides have been shown to be effective adsorbent materials [24]. Metal oxides likely experience electrostatic interactions with charged metal ions as the primary drive for the adsorption mechanism. The adsorbent materials charge, and therefore their ability to interact with a given pollutant is highly dependent on pH, an

example is iron oxide. In fact, the surface may have more net positively charged groups in acidic solutions (such as $FeOH^+$) or more net negative or neutral groups in basic solutions (such as FeO^-). The overall surface charge of metal oxide particles allows for electrostatic attraction or repulsion of heavy metal ions. Previous works have seen success with iron oxide based materials for both As (III) and As (V) adsorbents in neutral solutions [24]. It has also been found that metal oxides, such as ZnO, can affect the membrane surface charge and hydrophilicity which relates to arsenic rejection in filtration [25].

Cellulose acetate (CA) is a very useful polymer for water filtration processes, having reasonable mechanical properties and thermal resistance [35]. Some of the advantages of using CA is its low cost, sustainability (being both biobased and conditionally biodegradable) [36], and easy processing. Cellulose acetate polymer has ester (slightly polar) and hydroxyl (polar) functional groups available on the surface as shown by Figure 3.1.

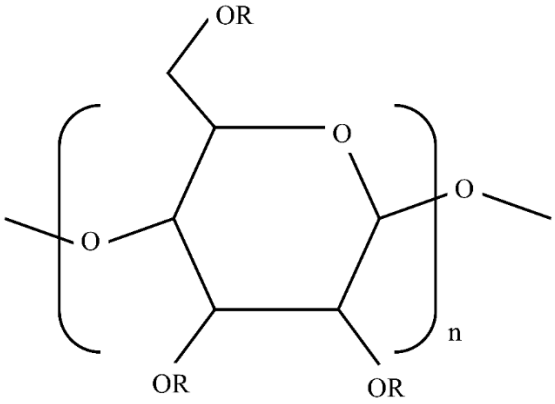

Figure 3.1 Basic chemical structure of cellulose acetate polymer (where DS=degree of substitution of acetylation) [37]

The degree of acetylation effects the polymers polarity and hydrophilicity, as it creates a higher ratio of the less polar acetyl groups. In the field of water filtration, CA is useful due to its insolubility in water and hydrophilic nature [35], hydrophilic membranes are less at risk for biofouling and enhance rejection of certain pollutants and encourage a high water flux [16]. Previous works which have electrospun cellulose acetate and composite metal oxide/cellulose

acetate fibers for various applications appear in Table S. 1 in Supporting Information as a non-comprehensive summary.

The review of the research shows that cellulose acetate is most successfully electrospun using a solvent mixture system with acetone, often Ac:DMAc, with polymer concentrations above 10 wt% in solution. The produced fiber diameters from literature range from 80 nm to 58 μm, often in the order of hundreds of nanometers.

Cellulose acetate blends are also commonly electrospun materials such as the electrospun mats produced by Pittarate et al. [54] who added small amounts of polyethylene oxide (PEO) to the CA polymer solution. These fibers used PEO to incorporate ZnO nanoparticles into the solution and achieved average fiber diameters for the different polymer blend ratios from 0.4 to 1.2 μm, and from 0.9 to 1 μm in diameter for the ZnO/polymer composite mats. In another paper by Luo et al. [55], they were able to create extra porous membranes for Cr(VII) removal by spinning a CA/polyethyleneimine blend and achieved an average fiber diameter of 4.3 μm.

In the work of Matos, Chaparro, et al. [27], the incorporation of metal oxide nanoparticles into electrospun fibers was shown to reduce fiber diameter, while in Hassan, Elkady, et al.,[48] it increased fiber diameter. These particles in cellulose acetate fibers have also been recorded to improve membrane integrity with better physical properties [27] and have better thermal stability than pure cellulose acetate [56].

A summary of the results of previous works with arsenic or microplastic removal using cellulose acetate membranes, with or without metal oxide additives are listed in Table 3.1.

Table 3.1 Literature review of relevant cellulose acetate membranes on microplastics removal and arsenic rejection

<table>
<tr><th>Work</th><th>Membrane composition</th><th>Production method</th><th>MP removal</th></tr>
<tr><td>Pizzichetti et al., 2021 [57]</td><td>CA membrane (5μm pore size)</td><td>Commercial product</td><td>Polyamide-20 μm average diameter particles-~100 % mass removed
Polystyrene-75 μm average diameter particles-~94% mass removed</td></tr>
<tr><td>Zhou et al., 2016 [47]</td><td>CA</td><td>Electrospun & hot pressed membrane</td><td>
<table>
<tr><th></th><th colspan="4">Particle size (μm) (Polystyrene)</th></tr>
<tr><th>Fiber diameter (μm)</th><th>5</th><th>2</th><th>0.5</th><th>0.1</th></tr>
<tr><td>0.96</td><td colspan="2" rowspan="2">~100%</td><td>77%</td><td>12%</td></tr>
<tr><td>1.3</td><td>28%</td><td>11%</td></tr>
</table>
</td></tr>
</table>

			1.57		32%	8%

Work	Membrane composition	Production method	Arsenic rejection
Durthi et al., 2018 [25]	CA	Phase inversion- solution cast 100 and 200 μm thickness	~30-40% removal
	Mixed membrane: 94wt% CA, 6% ZnO nanoparticles (diameter 50-500 nm)		~40-60% removal

While there are many cellulose acetate membranes produced by a variety of methods which investigated filtration of different pollutants [48] or in different media [58]. There aren't many cellulose acetate membranes in the literature that look at arsenic rejection and/or microplastic removal, as highlighted in Table 3.1. There were also some works which looked at water filtration using cellulose acetate blend membranes, for example the polyphenylsulfone (PPSU)/cellulose acetate membranes created by Kumar et al. in 2020 and 2021. They looked at PPSU/CA hollow fiber membranes with embedded ZrO_2 (2020) and ZnO-MgO (2021) particles and found arsenate rejection rates of 70-87% and ~80% respectively [59], [60].

The objective of this research is to create a water filtration membrane by solution electrospinning. A fibrous cellulose acetate membrane with embedded metal oxide nanoparticles will be used to remove arsenic and microplastics by filtration. This work is quite novel since microplastics is a relatively new field of investigation in terms of assessment and removal, while few works deal with arsenic and/or microplastic removal by cellulose acetate membranes. The produced membranes morphology and porosity are examined by scanning electron microscope (SEM) imagery and pycnometer based porosity measurements, respectively. Filtration capabilities of the membranes are evaluated by analysis of the feeds and filtration of the pollutant mixtures with inductively coupled plasma mass spectrometry (ICP-MS) for the measurement of arsenic concentrations in solution and microscopy to evaluate plastic particle size distributions in suspensions.

3.3 Methodology

3.3.1 Materials

The chemical species used in the electrospinning process include cellulose acetate (Sigma Aldrich 180955) with a degree of acetylation of approximately 40% and a number average molecular weight of ~30,000, magnetite (iron (II, III) oxide mix) nanoparticles (I.O. NPs) with 50-100 nm

diameters (Sigma Aldrich 637106), zinc oxide (SkySpring Nanomaterials 8410DL) nanoparticles (ZnO NPs) with 10-30 nm diameters, N-N dimethyl acetamide (sigma Aldrich D137510), and acetone (99.5%).

Arsenic (V) (Sigma Aldrich 76686) in water was used to simulate inorganic arsenic in groundwater for filtration tests. While inorganic arsenic exists in both (V) and (III) states commonly in groundwater, (V) is the less toxic state [10] and so is used for testing in this experiment. $CaCO_3$ was used to simulate natural water hardness levels in the solutions.

3.3.2 Electrospinning

Several conditions for electrospinning were varied in order to optimize the processes and produce smooth cylindrical fiber morphologies in the electrospun mats. Tested variables included polymer concentration in solution, solvent ratios, box humidity, spinning voltage, collector plate type, plate to needle distance, and solution flowrate. The optimized electrospinning conditions were used for the production of the tested membranes. The electrospinning setup is sketched in Figure 3.2.

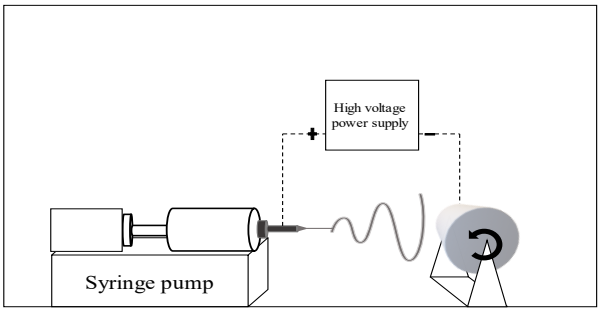

Figure 3.2 Sketch of electrospinning setup

3.3.2.1 Solution Preparation

The membrane spinning solutions were prepared by placing the solids in 3:1 acetone:DMAc solvent system according to the ratios described by Table 3.2.

Table 3.2 Electrospinning solution compositions

Membrane Short Name	**Solid species mass fractions**			**Solution concentration (wt% of CA in solvent)**
	Cellulose Acetate (CA)	Iron oxides (I.O.)	ZnO	
CA	1	0	0	17

0.5% I.O.	0.995	0.005	0	20
1% I.O.	0.99	0.01	0	20
2.5% I.O.	0.975	0.025	0	20
5% I.O.	0.95	0.05	0	20
ZnO	0.975	0	0.025	20
Mixed	0.975	0.0175	0.0175	20

All solutions were mixed then left to dissolve overnight with a magnetic stir bar set at 600 rpm. Solutions incorporating metal oxide nanoparticles (all but the neat CA) were sonicated for 30 minutes directly prior to electrospinning using a *Fisherbrand M2800* ultrasound bath..

3.3.2.2 Electrospinning conditions

The electrospun mats were spun for 6 hours each using a solution flow rate of 0.75 ml/h, and a 21 gauge needle. The collector plate used was tinfoil on a mandarin rotating at 60 rpm, ad was placed 10 cm away from the needle tip. The electrospinning box operated at room temperature (20-22 ºC), the humidity was controlled between 55-65% humidity, and a 22.5 kV potential was applied to the system.

3.3.2.3 Membrane preparation

The electrospun mats were heat treated by placing them in a distilled water bath at 90ºC for 45 minutes. Heat treatment of the mats allowed for cross points to be welded, decreasing pore size by decreased porosity and improving membrane durability (linked to tensile strength and chemical and physical stability) [19], [23]. In order to use the electrospun mats for the filtration application, they were removed from their collector foil, folded into 4 layers and shaped into 47 mm diameter disks to fit in the *Amicon* stirred cell (described below).

3.3.2.4 Sample analyses

Analysis of the electrospun mats was done mainly by SEM imaging. A *TM3030 Plus Hitachi* scanning electron microscope (SEM) was used to determine morphology and measurements of fiber diameter were made possible by processing the images with the software ImageJ. Approximately 500 measurements were taken per sample from SEM images. The porosity of the membranes used for filtration testing were calculated through the use of an *AccuPyc II 1340* pycnometer. The pycnometer calculated the average density of each fiber mat according to the

weight as measured by a scale and the volume determined from pressure differentials. This was related to the known density of the materials to determine membrane porosity. The average pore size of the mats was determined by the equation outlined by Eichhorn and Sampson [63] which related porosity and fiber diameter to pore size from empirical models.

The mean pore size of the membranes was estimated from the correlation in Equation 1 relating porosity and fiber diameter to pore size within a reasonable degree of accuracy.

$$r_{pore} = \frac{\sqrt{\pi}}{4} * \frac{\pi}{2\log\left(\frac{1}{\epsilon}\right) - 1} * d_{fiber} \qquad \text{Equation 1}$$

Where r_{pore} is the number average pore radius (μm), ε is the membrane porosity, and d_{fiber} is the number average fiber diameter of the mat (μm).

The measurements of the membrane morphologies were taken from different areas of the electrospun mats from which the membranes were made. The average values of these measurements were taken to represent the membrane morphologies of a given composition.

3.3.3 Filtration Tests

The filtration setup is shown in Figure 3.3, where a *Masterflex L/S* peristaltic pump was used to feed the desired flowrate to a 50 mL *Amicon* stirred cell filtration unit (with the stir bar removed to prevent membrane tearing) which was used to house the membrane. For gravity filtration tests, an initial volume of feed was added to the *Amicon* cell, and gravity induced flow at atmospheric pressure was used to drive filtration. In any filtration test, the first 3 to 5 mL of filtrate (≈ 1.7-2.9 L/m^2) were sent to waste to avoid contamination of the filtrate with residue on the membrane from the preparation process.

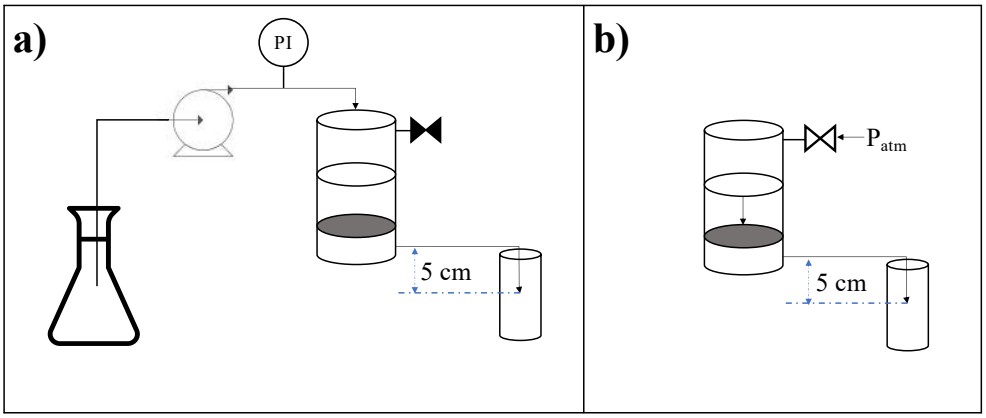

Figure 3.3. Filtration equipment setup for a) constant flow rate filtration and b) batch-fed filtration.

The approximate water flux of the constant flow filtration setup was ~21 $\frac{L}{m^2 \cdot h}$ and gravity filtration had varying flow rates with average flux of approximately 60 $\frac{L}{m^2 \cdot h}$ for all membranes. These flux values were measured from outlet flow rates and membrane dimensions. Very low pressure buildup (<1 inches of water) was measured by the in-line pressure gauge in the constant flow filtration setup in all filtration scenarios.

All filtration tests were performed but a single time due to time constraints. Any error values presented in the results relates to the deviations between multiple measurements of the same sample.

3.3.3.1 Arsenic (V)

Surplus iron oxide embedded membranes (~2 wt% I.O.) were used to conduct preliminary tests to choose the optimal conditions for arsenic filtration. The same membrane compositions were tested for arsenic rejection at three feed concentrations (100, 50, and 20 µg/L of arsenic (V) in water). Comparisons were also done between different membrane preparation methods, single layer, multilayer, and heat treated membranes were compared. These preliminary results showed that the best rejection was achieved by heat-treated membranes at 20 µg/L feed concentration, no difference was observed between the number of mat layers used for the membrane yet tearing more easily occurred in single layer membranes and so a multilayer setup was used for the rest of the study.

3.3.3.1.1 Filtration tests

A solution of 20 µg/L of arsenic (V) in Millipore water was prepared for use as the filtration feed by dilution of the stock solution. Arsenic feed solutions had a pH of approximately 7+/- 0.5 as measured by pH paper, and natural water hardness was simulated by adding calcium carbonate to the solution at a concentration of 150 mg/L $CaCO_3$ /L [64]. The addition of $CaCO_3$ caused solution turbidity and so the feed solution was agitated with a magnetic stir bar at a rate of 300 rpm to keep the feed composition consistent. The filtration conditions determined by the preliminary tests were used to investigate and compare the success of the final membranes for arsenic filtration. The constant flowrate filtration setup was used for these tests as shown in Figure 3.3. Samples were filtered for 25 to 30 minutes to produce 10 to 15 mL of filtrate solution for testing.

3.3.3.1.2 Adsorption tests

Arsenic adsorption behaviour was also tested for one of the membranes, in order. This was done to confirm the method of composite membranes' ability to adsorb arsenic and confirm adsorption as the rejection mechanism by the membrane. This test was done by placing a 5% I.O. membrane in 30 mL of 20 µg/L As(V) solution in a closed glass vial with no stirring. 15 mL of the solution was removed after 5 hours, and the remaining 15 mL were transferred to a sample vial after removal of the membrane after 24 hours.

3.3.3.1.3 Sample analysis

Arsenic (V) concentrations in both the feed and filtrates were determined by ICP-MS analysis by a *Perkin Elmer NexION 300x* device with an As detection limit of 0.004 µg/L.

3.3.3.2 Microplastics

3.3.3.2.1 Experimental preparation

For the investigation of microplastic filtration by the membranes, microplastics were created by physical fragmentation with the use of a mechanical blender. Rigid polystyrene (PS) taken from household packaging was placed in tap water and blended until there were just fine particles left in view and there was obvious turbidity in the solution. Using common household plastics of varying particle size allowed for the experiment to reflect real world incidents of microplastics pollution and use recycled materials for these tests.

Gravity filtration of a set volume was used to evaluate microplastic removal from water as the piping was too fine through the peristatic pump to allow most of the microscale or macro scale plastics to pass to the filtration cell. Therefore a set volume of 20 mL of the plastic in water mixtures was added to the *Amicon* cell and the driving force for filtration was gravity alone, with the outlet from the cell approximately 5 cm above the inlet to the filtrate receptacle.

3.3.3.2.2 Sample analysis

Microscopy was used to analyse the size distribution of the plastic particles in the feed and filtrate mixtures. An *Olympus BX51* microscope was used for image taking, where a small volume of water from a given sample was imaged in 5-10 different areas, and these images were then analysed with the use of ImageJ software. Approximately 500 to 1000 plastic particles were evaluated per sample depending on the particle concentration in the suspensions.

3.4 Results and Discussion

3.4.1 Morphology

3.4.1.1 Resultant Membranes

The SEM images of the final electrospun membranes with compositions and labels described in Table 3.2 are shown in Figure 3.4.

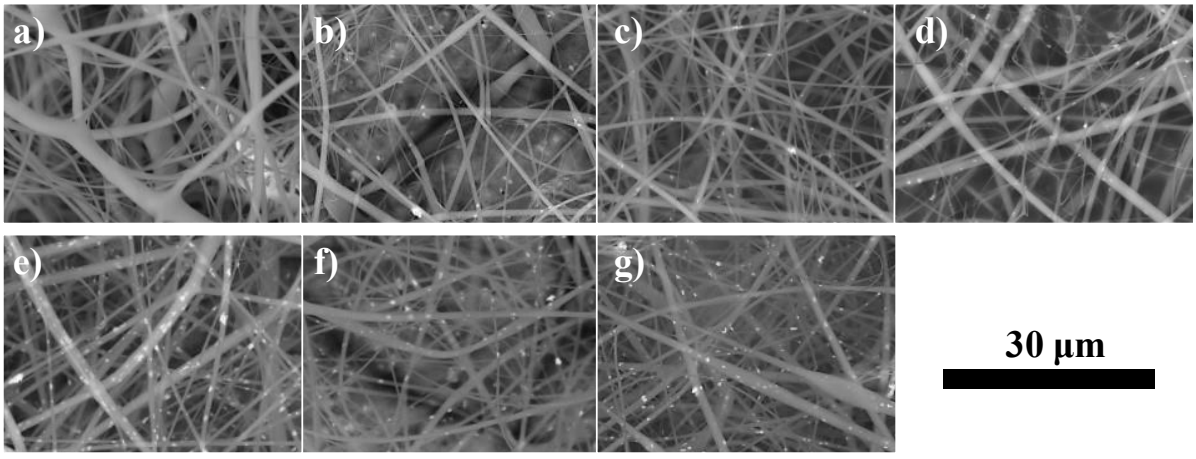

Figure 3.4 SEM Images of membrane morphology. The membranes are presented in the order a) CA b) 0.5 wt% I.O. c) 1 wt% I.O. d) 2.5 wt% I.O. e) 5 wt% I.O. f) ZnO g) Mixed.

Qualitative analysis of the membranes shown in Figure 3.4 show that smooth cylindrical fibers were obtained for the vast majority of the membranes; however, some defects can be seen in lower magnification images, where some elongated beads can be seen amongst the fibers. The fiber diameters are not uniform for any of the membranes, Figure 3.5 shows an example of the fiber diameter distribution of a membrane.

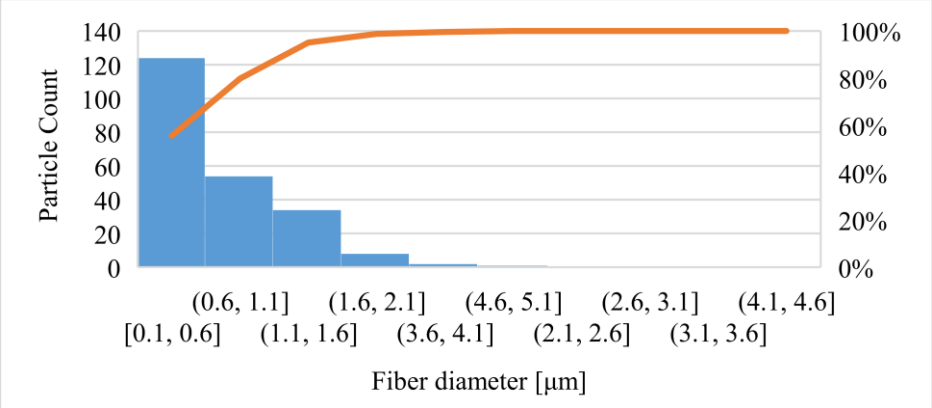

Figure 3.5 Histogram of fiber diameters of the CA membrane

As shown by Figure 3.5 the majority of fibers in the neat CA membrane have diameters between 0.1 and 0.6 µm, and much fewer fibers of higher diameters were observed.

The metal oxide nanoparticles can be observed in Figure 3.4b through g as the bright white dots within the polymer fibers. Agglomeration of the metal oxide nanoparticles is therefore evident in the samples as the visible metal oxide particles are significantly larger in size (particle diameters shown to be around the fiber diameter in the images ~0.5 um) than the known nanoparticle diameters (50 nm for I.O. and 20 nm for ZnO) before being placed in the polymer suspension. Therefore, the bath ultrasound seems insufficient for optimal dispersion of nanoparticles in the polymer solution or is negated by re-agglomeration of the particles during the spinning process. However, preliminary tests showed an improvement in nanoparticle dispersion and distribution with ultrasonication, and no significant improvement was observed with increased sonication time above 20 minutes. Matos, Chaparro, et al. [27] also found agglomeration of metal oxide nanoparticles in their fibers electrospun with the nanoparticles in solution, yet no sonication was indicated in their process. This nanoparticle agglomeration likely affected the membrane's mechanical properties and adsorption capabilities compared to well dispersed composite membranes.

3.4.1.2 Membrane processing

Preliminary tests showed membrane performance for arsenic removal and durability after heat treatment. The nonwoven mats were therefore annealed before filtration tests, an image of a membrane before and after processing can be seen in Figure 3.6.

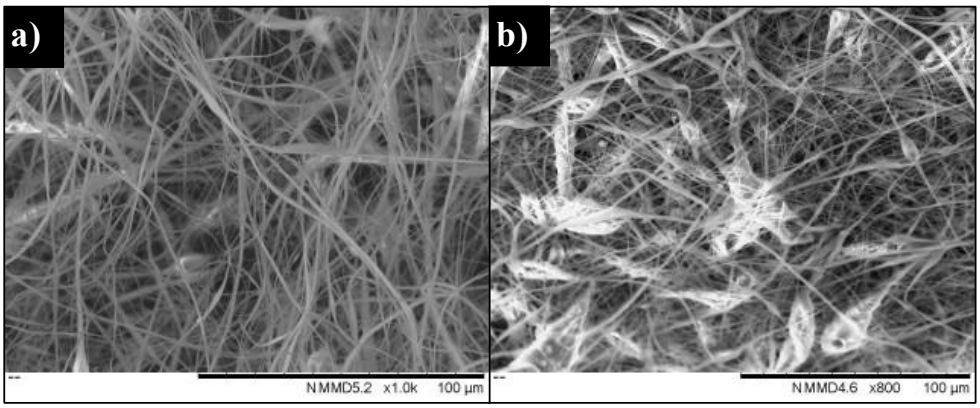

Figure 3.6 Effect of neat CA membrane annealing on fiber density a) before annealing b) after annealing

Membrane annealing increased the fiber density of the mats, as can be seen by comparing images a and b in Figure 3.6. At junction points, fibers are adhered together after heat treatment causing higher fiber density areas. The morphological difference observed between the two images shows a clear effect of the heat treatment method used on the fiber mats. Although the fiber density was altered, image analysis of the mats before and after heat treatment showed no significant difference to fiber diameter after processing.

3.4.1.3 Quantitative analysis

To represent the fiber diameter distribution of all produced membranes the number and volume average fiber diameters are shown in Figure 3.7.

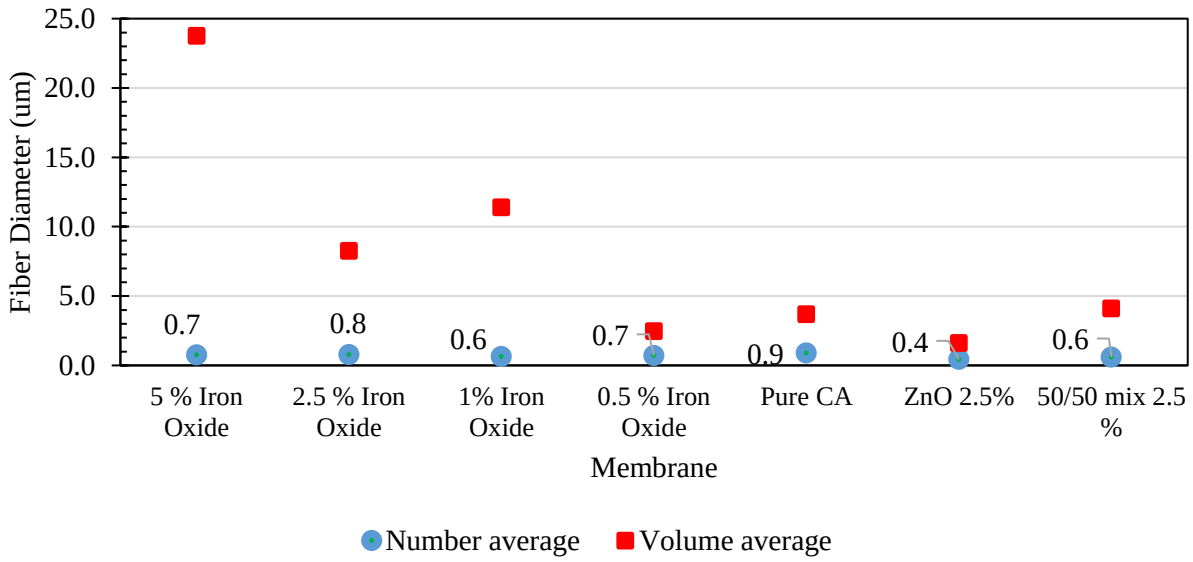

Figure 3.7 Summary of electrospun mat fiber diameters, where the number average fiber diameter values are indicated next to their data points

As shown by Figure 3.7 the average fiber diameter for the samples ranges from 0.4 to 0.9 µm, however there is no significant difference between mean fiber diameters according to two-tailed t-tests with a significance levels (α) of 0.05. The volume average fiber diameters are shown to represent the varying polydispersity between membranes. Number average fiber diameters are the direct average of diameter measurements. A volume average fiber diameter is the sum of all diameter measurements to the power of four divided by the sum of the diameters to the power of three, this method of calculating mean diameter provides a value which is more representative of the average diameter in terms of how much volume each fiber occupies. No significant difference of fiber diameters was observed between membranes; however it is clear that the fiber uniformity relies on membrane composition. Higher polydispersity is observed with higher concentrations of I.O. nanoparticles, likely due to higher solution viscosity and additive agglomerations causing irregularities during spinning. The lowest polydispersity, with the smallest fiber diameter was observed in the ZnO embedded membrane. This is likely explained by a higher conductivity of the electrospinning solution with ZnO additives improving the drawing force in electrospinning [53]. The slight difference between the fiber diameters in the I.O. and ZnO embedded membranes of the same concentration can be explained by the nanoparticle size, the I.O. nanoparticles had larger particle size than the ZnO NPs causing more irregularities at the same additive concentration.

The porosities were calculated from pycnometer measurements and the estimated pore size of each membrane are shown in Figure 3.8.

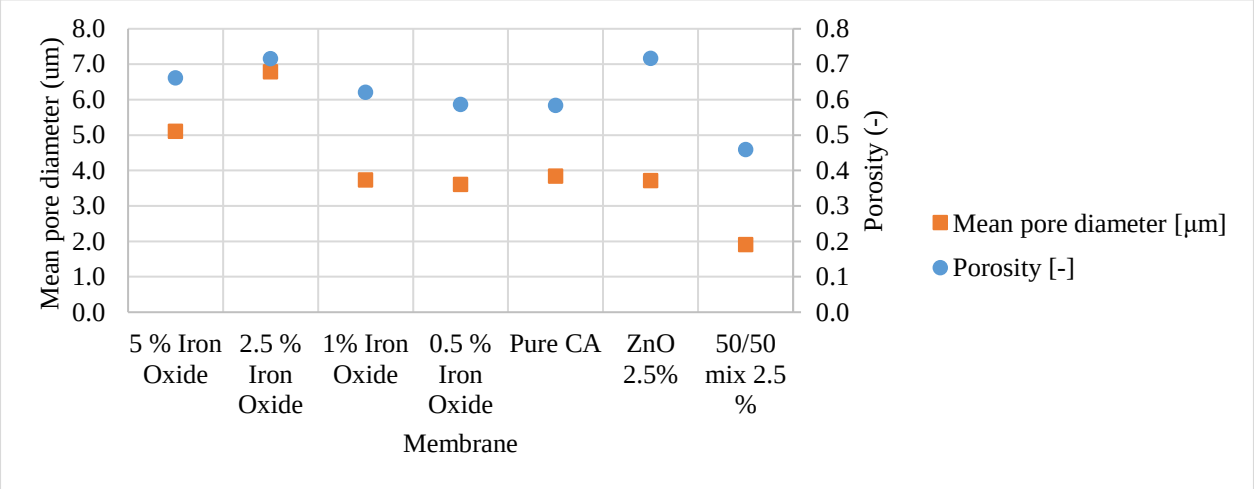

Figure 3.8 Plot of pore size and porosity of membranes used in filtration

The porosity of previously electrospun cellulose acetate mats have been found in the range of 65 to 85 % porosity [47]. Figure 3.8 shows the porosity of the CA membranes to be between around 50 to 70%, which is slightly lower than the porosity determined in previous works, this is likely an effect of the membrane heat treatment increasing fiber density and causing a slight decrease to porosity. These mats also have pore sizes from 2 to 7 µm in diameter, with the lowest pore size and porosity belonging to the mixed membrane. A certain amount of error can be expected in these results as the pycnometer results provided a standard deviation for 50 measurements of up to 10% of the final average. The calculated pore sizes must be accepted as estimations as they are empirically calculated from multiple measurements with their own associated error (porosity, fiber diameter), however these results agree with the findings presented below. The mean pore sizes were calculated based on number average fiber diameter, however according to the pore size modelling done by Nakamura et al. [65], the pore size distribution varies proportionally according to the mean fiber diameter in non uniform membranes.

3.4.2 Filtration Tests

3.4.2.1 Arsenic (V)

The membranes were tested with a feed concentration of 20 µg/L of arsenic in Milli-Q water (Millipore, USA) (pH of 6.998) [66]. Unless otherwise noted, the tests were done using a flow rate

of 0.6 ml/min at a temperature of 21 ºC (room temperature), the contact time was estimated to be between 0.4 to 1.5 seconds as calculated from known mat thickness and flux. The arsenic rejection for each sample is listed in Table 3.3 where rejection is defined as the percentage of arsenic removed from the feed to the filtrate [25].

Table 3.3 Arsenic rejection by membranes during filtration with filtrate concentration from 5.6 to 20 µg/L of As(V)

Membrane	**Arsenic (V) Rejection (%)**		
CA	51.82%	±	0.77%
I.O. 0.5%	0%	±	-0.19%
I.O. 0.5% (Q=2 ml/min)	0.80%	±	0.01%
I.O. 2.5%	69.21%	±	1.10%
I.O. 5%	48.08%	±	0.94%
ZnO	45.12%	±	0.96%
Mixed	9.85%	±	0.15%
Mixed (T=35dC)	10.74%	±	0.18%

In the previous study of Potla Durthi, Rajulapati, et al. [25], arsenic rejection rates of CA membranes ranged from 30 to 60 %. In comparison to Table 3.3, CA, I.O. 2.5%, I.O. 5%, and CA/ZnO showed similar rejection rates. Only the I.O. 2.5% membrane performed better than plain CA fibers for arsenic rejection, showing that there is an optimal metal oxide additive concentration in order to improve membrane performance, while additive contents away from the optimal value simply disrupts the CA surface polarity. It should be noted that the particle size and distribution of the metal oxide nanoparticles (or their agglomerates) would also impact the surface polarity.

Cellulose acetate is a hydrophilic and polar polymer [35], the polarity of its surface allows for selective permeation of water molecules and therefore arsenic rejection [16]. The introduction of metal oxides, which can have variably charged surface groups, is an ideal asset to promote adsorption. However, the presence of these particles likely alters the net polarity/hydrophilicity of the membrane or its polarity distribution by interacting with the polar surface groups of the cellulose acetate polymer matrix [24]. However, the PPSU blends with metal oxides made by Kumar, Isloor, et al. [59], [60] showed arsenate oxide (an inorganic arsenic state) rejection rates of around 80%. It would be interesting to see if the rejection of other arsenic forms by the membranes differs from the findings in this work, or if the improved rejection by Kumar et al. is due to membrane material and morphology.

The adsorption capabilities of the 5% I.O. embedded membrane was tested after 5h and 24 h using the same initial solution concentration as for filtration (Figure 3.9).

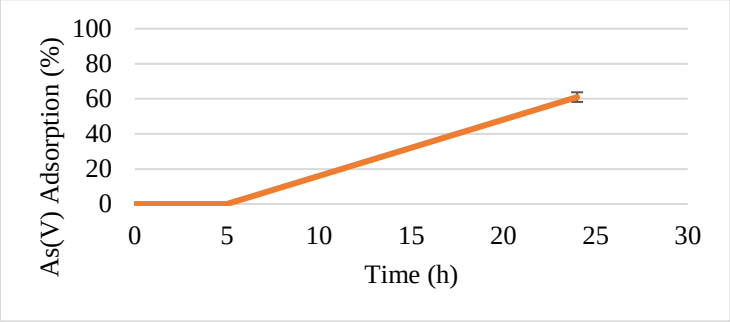

Figure 3.9 Arsenic adsorption by 5% I.O. embedded CA membrane

Figure 3.9 shows that the membrane with embedded metal oxides shows some promise for a fixed bed type adsorption material, with the ability to remove 61% of arsenic from a 20 µg/L arsenic in water solution after 24 h. No adsorption was observed in the first 5 h, yet the same membrane was able to reject 48% of the arsenic feed in filtration with a contact time of a few seconds. This is possibly because the mass transfer of arsenic in stagnant adsorption differs from that of permeate flow, allowing arsenic ions to reach available adsorption sites much more quickly in pressurized filtration. The differing arsenic rejection between membrane types may therefore be due to the effects of the surface charge throughout the fiber network on permeate flow patterns. Investigation of the adsorption mechanisms of the mats may be an interesting avenue for future work.

3.4.2.2 Microplastics

3.4.2.2.1 Particle size distributions

The microplastic particles in the feed and filtrate water suspensions were analysed by microscopy and image analysis. Figure 3.10 shows the particle size distribution of the PS particles in water before and after membrane filtration.

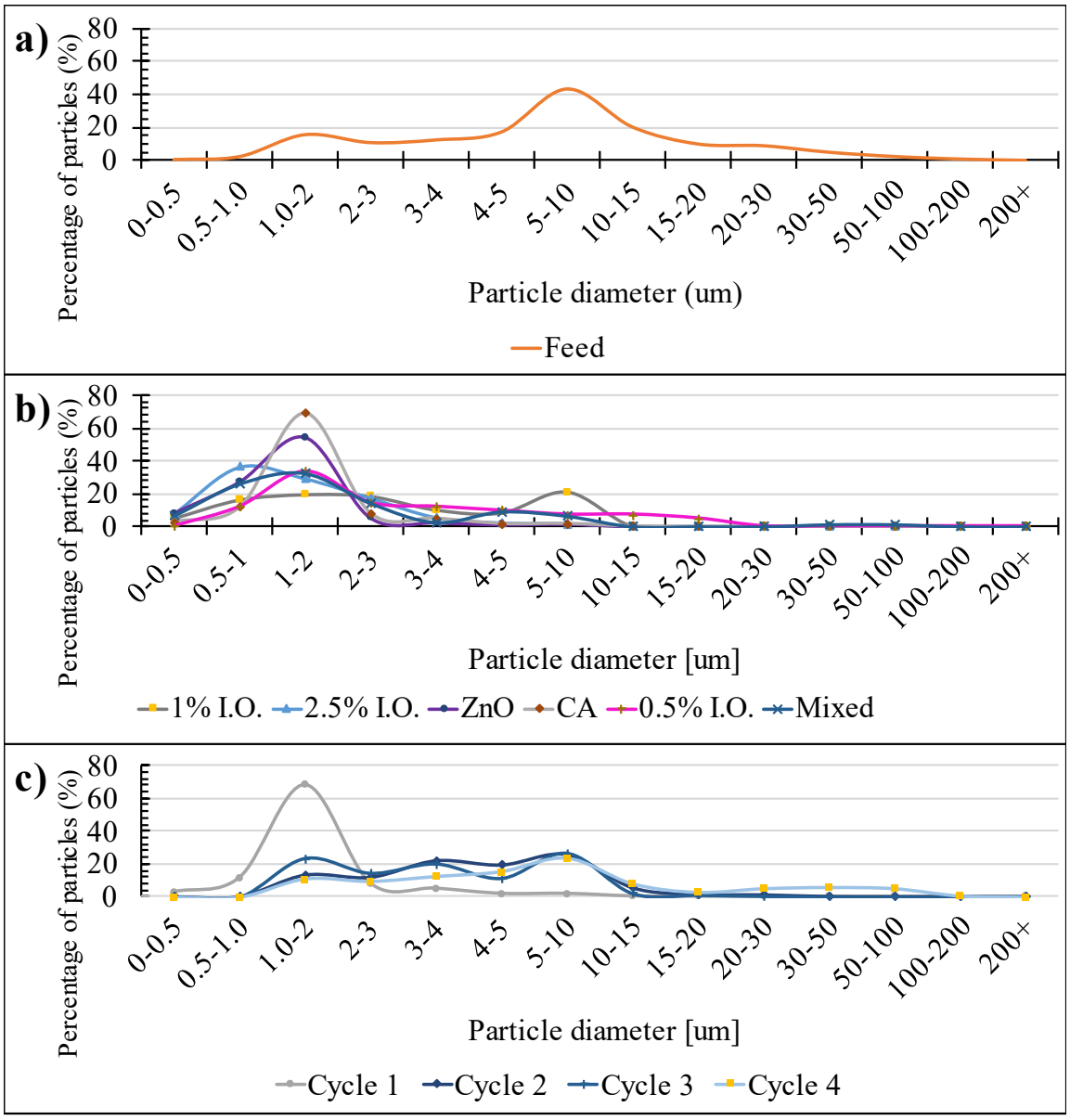

Figure 3.10 Microplastic particle size distributions of a) the feed suspension, b) the filtrates after filtration by different membrane compositions, and c) the filtrates after filtration by neat CA membranes over multiple filter-rinse cycles

3.4.2.2.2 Microplastic production

Figure 3.10 a) shows that microplastics particles had median and average diameters of around 6 and 10 μm respectively, with particles ranging from 0.3 μm to 500 μm in diameter. A vial of the microplastic suspension feed is shown in supporting information (Figure S.1) the slight opacity of the feed made evident that there was a sucessful suspension of plastic particles at a sufficient concentration (~1000 particles/mL) to allow for filtration analysis by microscopy. This feed was be useful in investigating the membranes' capabilities, however was not representative of real world conditions. The resolution of the microscope imaging process varied; the presence of larger particles interrrupted the microscope's ability to observe the smaller particles in suspension. Based on images of the filtrate suspensions, more plastic particles with diameters below ~3 μm were observed for the same volume of water than were observed in the feed samples, we can therefore conclude that the count of particles was skewed towards larger particle diameters. Examples of microscopy images can be found in supporting information (Figures S.2 and S.3) to provide insight on how the particles were analysed. To help better understand the data, filtrate particle size distributions were analyzed alongside particle removal, allowing for more accurate comparisons between filtrates and between filtrate and feed supensions to be drawn.

3.4.2.2.3 Rigid polystyrene filtration

Figure 3.10 b) shows that all membranes effectively removed most particles above 20 μm in diameter, with very few particles above 10 μm making it through the ZnO, CA and 2.5% I.O. membranes. All but the 1% I.O. membrane show very similar particle size distributions (with the 1% I.O. membrane having more particles between 5-10 μm in their filtrate), and so based only on these curves there is little to suggest any significant difference between the performance of these membranes for microplastic removal. These results agree with the pore size estimations shown in Figure 3.8. The average pore sizes of the membranes are between 2 and 7 μm in diameter, however the pore size varies within the membrane, likely according to a pseudo-normal distribution curve [65], meaning that some particles above the pore size can make it through. Comparing the filtrate distributions to the feed distribution (Figure 3.10), it is clear that most particles having a size above the average membrane pore size were removed with very few outliers with diameters above the pore sizes being able to pass through the membranes. The comparisons of the filtrate to the feed particle size distributions are summarised in Table 3.4 in terms of percent removal.

Table 3.4 PS particle removal by CA and composite membranes based on particle count

	Particle diameter [µm]					
Membrane	**<10**	**10-15**	**15-20**	**20-50**	**50-100**	**>100**
0.5% I.O.	0%	0%	0%	100%	100%	100%
1% I.O.	0%	0%	0%	100%	100%	100%
2.5% I.O.	0%	100%	100%	100%	100%	100%
ZnO	0%	24%	100%	100%	100%	100%
Mixed	0%	100%	100%	0%	0%	100%
CA	0%	0%	100%	100%	100%	100%

Table 3.4 shows effective removal by the membranes of particles having a size above 15 µm. There are some discrepancies compared to the qualitative analysis between the feed and filtrate compositions as shown by the particle size distributions. This is likely due to the need to normalize the size distributions according to particle count because of the varying microscope resolution, causing more weight to be attributed to larger particles in the filtrate suspensions than is necessarily representative of reality. For example the mixed membrane filtrate samples showed but 1 particle each in the 50 and 100 µm size bins, yet once normalized the results showed no effective removal by the membrane. Once again, no significant difference between membrane performance is observed, showing that the pore sizes, like the fiber diameters, do not vary significantly between the membrane compositions. One can therefore assume that in this work, the microplastic removal is purely based on physical morphology and not on membrane composition or surface charge.

One noteworthy observation from the microscopy filtrate analyses was the absence of particulate matter in the filtrate suspensions after membrane filtration with a blank feed. The membranes were tested for filtration with just water and the feed and filtrates analysed by microscopy, these tests revealed that no polymer particles (above the microscope's level of detection) broke off from the

membrane itself due to the filtration process. This suggests that the use of a polymeric membrane does not contribute to the microplastic contamination of the filtrates.

3.4.2.2.4 Membrane Reusability

The distributions shown in Figure 3.10 c) make it clear that after just one rinse cycle the membrane begins to lose its integrity, allowing more particles from 3 to 15 µm to pass through. The effective removal rates compared to the feed suspension are shown in Table 3.5.

Table 3.5 PS particle removal by CA membrane over multiple filtration cycles based on particle count

	Particle diameter [µm]								
CA Cycle	**<2**	**2-5**	**5-10**	**10-15**	**15-20**	**20-50**	**50-100**	**100-200**	**200+**
Cycle 1	0%	55%	94%	98%	100%	100%	100%	100%	100%
Cycle 2	0%	0%	11%	44%	74%	86%	100%	100%	100%
Cycle 3	0%	0%	8%	76%	78%	93%	100%	100%	100%
Cycle 4	0%	0%	18%	16%	49%	0%	0%	0%	100%

Table 3.5 shows that the cut-off diameter for removal above 90% by the cellulose acetate membrane moves from 5 µm at the first filtration to ~50 µm, to ~20 µm, to over 100 µm after 4 cycles. The drop in membrane effectiveness is likely due to abrasion of the membrane by the microplastics during rinsing. SEM imaging of the PS particles on the membrane (Figure 3.11), showed them to have clean angular edges from the mechanical cutting, and showed them embedded in the fibers.

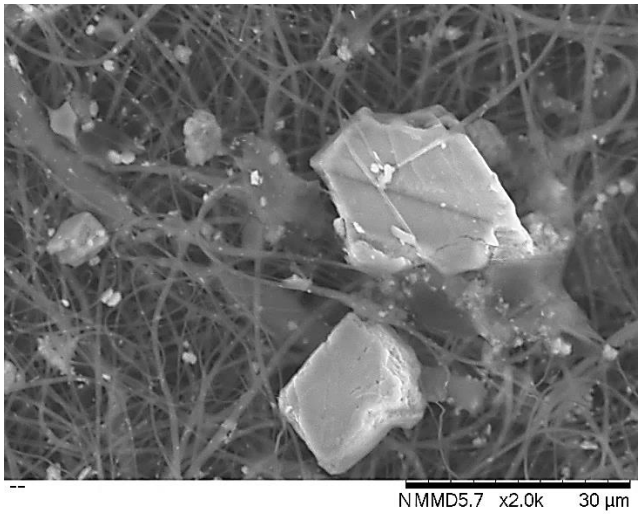

Figure 3.11 SEM image of Mixed membrane after plastic filtration

It is feasible that they could tear the membrane during removal. These results show that this membrane is not necessarily suited for reusability past one or two cycles in plastic filtration, as the fourth filtrate begins to allow particles near the macro scale to pass through.

3.5 Conclusion

This work successfully electrospun seven different membranes made of cellulose acetate with varying compositions of both iron oxide and zinc oxide nanoparticles. The membrane morphologies did not significantly differ from one another in fiber diameter, the average pore sizes of the membranes varied from 2 to 7 µm. The membranes performance for arsenic removal succeeded in comparison with previous literature. The most successful membrane was the 2.5% iron oxide embedded membrane performing at around 70% arsenic rejection while the neat cellulose acetate membrane was the second best performing with around 52% arsenic rejection, while the addition of metal oxides in the ZnO, Mixed, and I.O. 0.5%, and 5% membranes only worsened rejection performance. Further investigation of the composite membranes with more incremental composition changes can be done to manipulate the surface charge distribution of the membrane and obtain optimal rejection.

These membranes succeeded at removing microplastic particles above around 5 to 10 µm in diameter and could be used for basic microfiltration. Metal oxide nanoparticles in the fibers did not

have any noticeable impact on microplastic removal and so plastic filtration can be attributed primarily to membrane morphology.

In conclusion, we can see that in terms of arsenic and microplastic filtration, there is not necessarily a significant reason to include metal oxide nanoparticles in the electrospun membranes as the neat cellulose acetate membrane performed well in both cases. However, further research into the mechanical properties of the composite membranes may support their use in water filtration.

CHAPTER 4 ADDITIONAL METHODS AND RESULTS

This chapter expands on the research presented in Chapter 3 previous. Some results were excluded from submission to publication for brevity, such as the preliminary electrospinning results, and filtration of low density polyethylene (LPDE) MNPs. The analysis of copper (II) removal by the membranes was neglected for the article due to the high error of the measurement process of copper (II) ions. The following sections list these methods and results with reference to findings presented previous, to show the full scope of the research.

4.1 Electrospinning Optimization

4.1.1 Methods

Prior to the electrospinning of the final mats shown in Figure 3.4 for filtration testing, multiple electrospinning conditions were tested to optimize fiber morphology. Table 4.1 lists all the variables tested in considering the final electrospinning conditions.

Table 4.1 Summary of conditions tested in electrospinning optimization of CA and composite mats

Condition varied	**Units**	**Tested Range**
CA concentration in solution	wt%	10-22
Applied voltage	kV	15-27
Solvent system ratio	Acetone:DMac	1:0 to 1:2
Tip to collector distance	cm	5-20
Collector type	-	Plate, Mandarin (20-100 rpm)
Metal oxide concentration	wt% of CA	0-15
Syringe flow rate	mL/hour	0.25-1.5
Relative humidity	%	40-70

Solutions for testing were prepared according to the methodology described in 3.3.2.1, and the samples were spun for 20 minutes each to provide basic information on fiber morphology using a given set of conditions. The influence of nanoparticle concentration was addressed in Chapter 3, and there were no noticeable differences between samples when voltage, collector type, or tip to collector distance were varied and so these results were not presented.

4.1.2 Results

4.1.2.1 Solvent system

Multiple solvent systems were tested at varying polymer concentrations, solvent ratios of higher DMAc (2:1 and 1:2 Ac:DMAc) did not form smooth fibers at their tested conditions. An example of the fibers produced by three of the solvent mixtures tested for 17% CA solutions spun at 1 mL/h and 22.5 kV are shown in Figure 4.1.

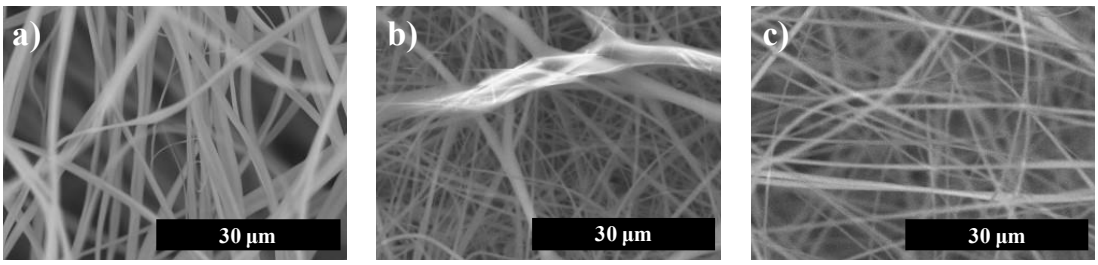

Figure 4.1 SEM images of CA mats spun using Ac:DMAc solvent systems with ratios of a) 1:0, b) 4:1, and c) 3:1

The use of a pure acetone solvent system allowed for smooth fibers to be spun, however they were collapsed into ribbon like structures as evident in Figure 4.1 a), likely due to the high volatility of the solvent. The addition of DMAc to the solvent system increased the vapour pressure, reducing the risk of needle clogging due to rapid evaporation and creating cylindrical fiber morphologies. Comparing b) and c) in Figure 4.1 one can see that the 3:1 Ac:DMAc system had more uniform fiber diameters than found using the 4:1 system. Given these results, a 3:1 Ac:DMAc solvent system was selected for further testing.

4.1.2.2 Flowrate

The solution flowrate from the spinneret is an important factor in determining fiber diameter. Figure 4.2 shows samples of neat CA and 9% I.O. membranes spun at varying flow rates using a 17% CA in 3:1 Ac:DMac solution with an applied voltage of 22.5 kV.

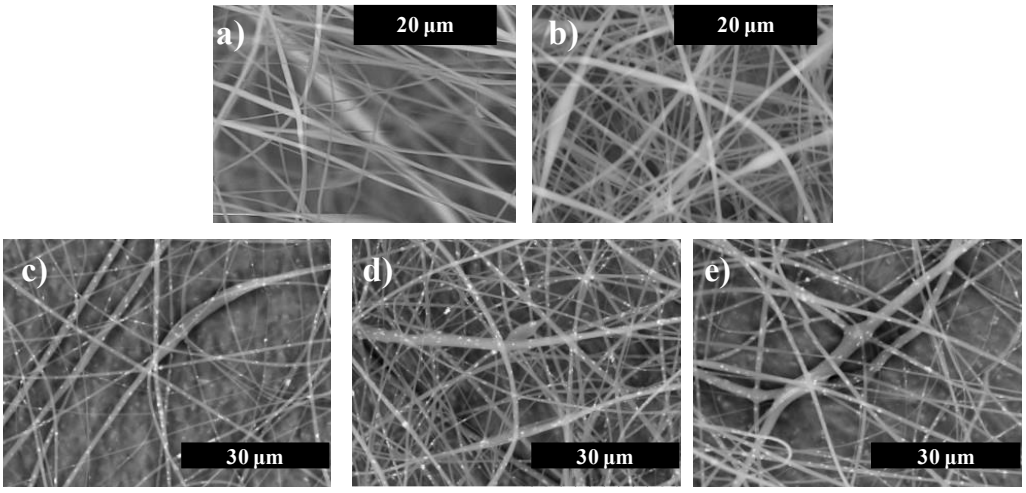

Figure 4.2 SEM images of neat CA membranes spun with flowrates of a) 0.75 and b) 1.25 mL/h and 9% I.O. mats spun at flow rates of c) 0.5, d) 0.75, and e) 1 mL/h

Figure 4.2 shows that too high flow rates can lead to elongated beads in the fibers due to spinning instabilities as shown by images b) and e). At a lower flowrate of 0.5 mL/h (c) the fibers are finer, however lower magnification images shows some broken fibers when there is insufficient flow. While there were no significant differences found in the average fiber diameters between samples by a quantitative analysis, the optimal fiber morphologies over multiple samples were found most often with flow rates of 0.75 mL/h. Therefore this flow rate was selected for final membrane production, producing the most uniform, cylindrical, bead free fibers.

4.1.2.3 Polymer concentration in solution

The concentration of polymer in solution in electrospinning must be high enough to allow for overlap and entanglement of the polymer chains during spinning to allow for fiber formation [40]. A range of CA concentrations in solution were tested based on the ranges seen in previous literature. Figure 4.3 shows fibers spun by various solution concentrations at a flow rate of 0.75 mL/h and a 22.5 kV potential difference.

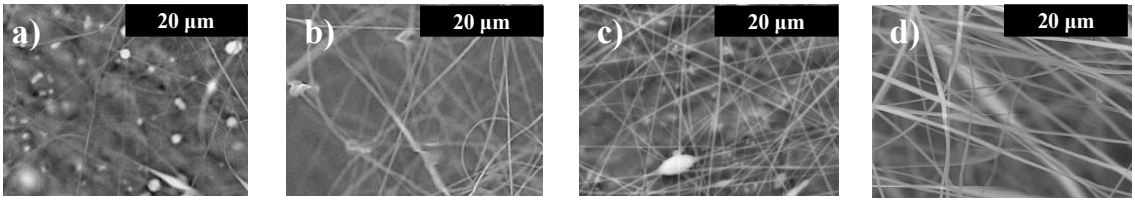

Figure 4.3 Electrospun cellulose acetate in 3:1 Ac:DMAc at polymer concentrations of a) 10 wt%, b) 12 wt%, c) 15 wt%, and d) 17 wt%

As shown by Figure 4.3 smooth cylindrical fibers were achieved at 17 wt% CA in solution, previous to that concentration, the mats are highly beaded with very fine polymer fibers connecting the beads. At concentrations above 17 wt%, the fiber diameters were seen to increase, and so 17% was chosen as the concentration for the final membrane solution in order to minimise fiber diameter while still maintaining a bead free morphology.

4.1.2.4 Effects of humidity

One of the most significant factors on the results was the humidity in the electrospinning box. Low relative humidity levels can lead to too rapid solvent evaporation creating thicker fibers and splitting instabilities. At too high relative humidity the solution jet solidifies after capillary instabilities have caused beading of the polymer fibers [67]. In the case of these experiments, the high volatility of the 3:1 Ac:DMAc solvent system means that high relative humidity levels are required for a stable solution cone and smooth fibers to be formed as seen in Figure 4.4.

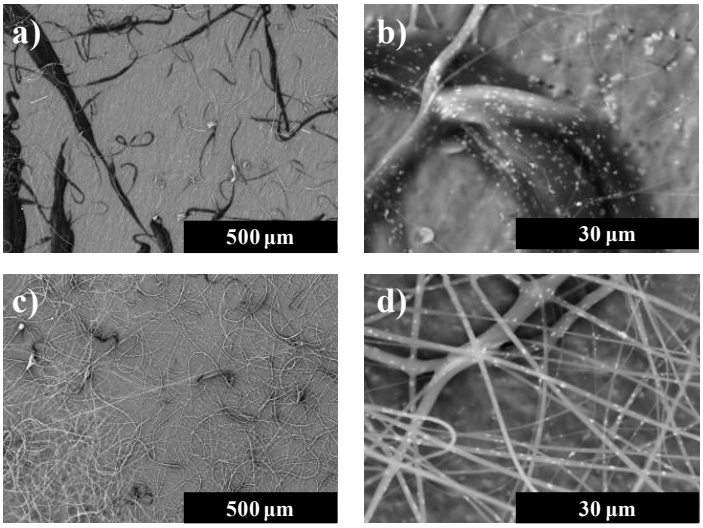

Figure 4.4. SEM images of 9wt% I.O. in 20% CA in 3:1 Ac:DMAc spun in 40% (a) and b)) and 70% humidity (c) and d))

As shown above, the humidity of the electrospinning box is a critical factor in the electrospinnability of the fibers given all other conditions are the same. The spinnability of samples during the winter months became much more difficult due to the high volatility of the solvent in

dryer conditions, the humidity had to be increased to a minimum of 55% ranging up to 65% to allow for the production of cylindrical fibers for all samples and final membranes.

4.1.2.5 Spinning time

The effect of spinning time on the fiber morphology can be seen by Figure 4.5, which shows a neat CA mat spun for varying time lengths where all other spinning conditions remained the same.

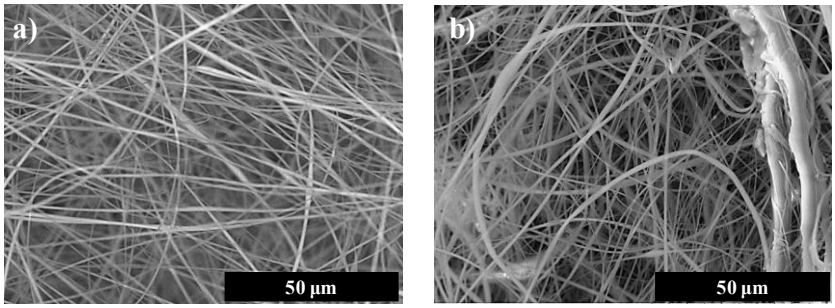

Figure 4.5 SEM Images of neat CA membranes after spinning times of a) 20 minutes and b) 6 hours

Increased spinning times led to the development of imperfections in the fiber mats. With long spinning times slight needle clogging began to be observed causing few thicker fibers to be deposited in the mat as shown by comparing the images in Figure 4.5. The imperfections at larger spinning times can also be attributed to a build up of polymer material on the collector reducing the conductivity of the collector plate and the electrostatic drawing force on the system.

4.2 Copper (2) Filtration

Copper (II) ions were used to test the metal ion removal capabilities of the membranes at higher concentrations (in the order of g/L) than reasonable in arsenic testing.

4.2.1 Methods

4.2.1.1 Experimental preparation

The copper (II) solutions were produced by dissolving copper (II) nitrate trihydrate (sigma-aldrich 61194) in Millipore water. The copper salts were massed using an electronic scale to obtain the appropriate amount of salt for the proposed copper ion concentration in water. Copper filtration was done using constant flow filtration (Figure 3.3) at a flow rate of 0.6 mL/hour. The pH of copper

(II) ions in water is around 4, as measured by pH paper. The pH levels of certain feed solutions were increased by adding incremental amounts of 1 molar NaOH solution until an increase of pH was detected.

Adsorption tests for copper were done by placing the membranes each in around 30 mL of 0.25 g Cu(II)/L aqueous solution, around 5 mL of solution was extracted from the samples at each of the measured times for later analysis.

4.2.1.2 Sample analysis

The concentration of copper (II) ions in solution were analysed with the use of an *Ultrospec 1100* UV/Vis Spectrophotometer. This was done using plastic disposable cuvettes, the absorbance of three 1 mL volumes of solution were measured for each sample, and the average absorbance was related to the concentration with the use of a calibration curve. The absorbance levels of the spectrophotometer were zeroed with distilled water before each individual absorbance measurement to avoid a baseline drift or variety caused by the use of different cuvettes.

4.2.2 Results

4.2.2.1 Calibration curve

The concentrations of the filtrate solutions were measured by relating concentration to absorbance using the function described by the calibration curve in Figure 4.6.

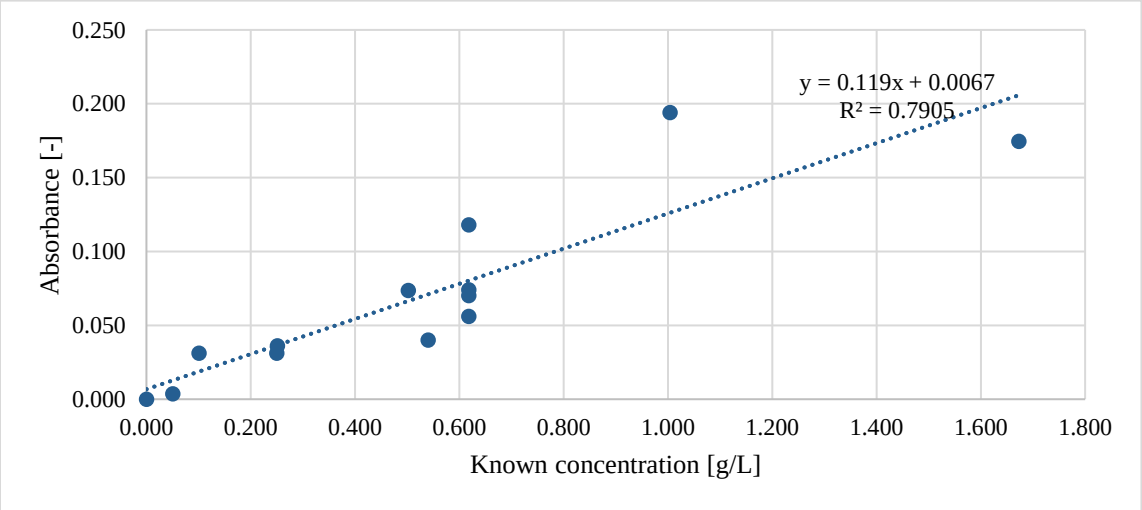

Figure 4.6 Relationship of absorbance against copper (II) ion concentration

The graph above shows that there is not a very strong relationship between ion concentration and absorbance, with a R value of only 0.79. This curve is therefore not acceptable for proper analysis of copper concentration and any results serve only as estimates of the true ion concentration. The low R value is likely due to the high variability in the absorbance values by the spectrophotometer. As seen by the data points in the graph, four different solutions of 0.6 g/L were measured for the calibration curve, however the absorbance results ranged from 0.056 to 0.118. The trendline seems to correlate better to the raw data in the lower end of the concentration range, and so feed concentrations of no more than 0.6 g/L were used in filtration tests to try to get more accurate results. Furthermore, the calibration curve measurements were taken only with copper (2) ion solutions (blue and transparent solutions) at a pH of around 4, yet the filtration tests were done over a range of pH values which altered the state of copper in solution as demonstrated in Figure 4.7.

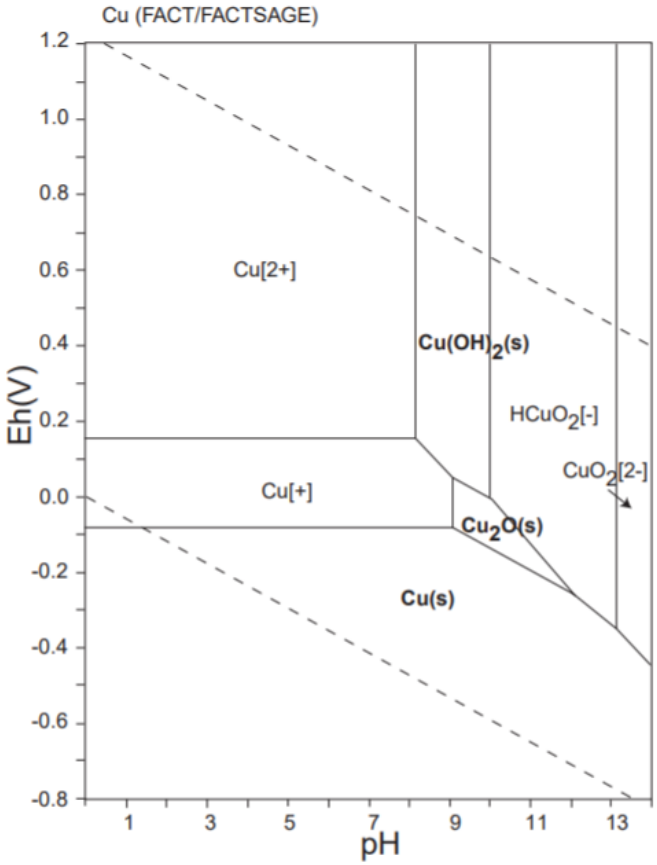

Figure 4.7 Eh-pH diagrams of the system Cu-O-H. $\sum Cu = 10^{-10}$, 298.15K, 105 Pa [68]

Figure 4.7 shows that for redox potentials above around 0.2 V, as was seen throughout the copper filtration tests, that for increasing pH values, the state of copper in solution goes from the Cu (II) ion to solid copper hydroxide, to negatively charged copper ions. Within the tested pH values only the state change from Cu(2+) to $Cu(OH)_2$ is observed.

Results for copper ion removal must therefore be taken with a grain of salt because of the high error in spectrophotometric results, especially concerning incremental changes in concentrations, as well as the inability for spectrophotometry to be used to ascertain the concentration of the solid copper state with any degree of accuracy.

4.2.2.2 Membrane type

The figures below look at the filtration of copper from different membranes. Figure 4.8 shows the concentration of Cu(II) ions before and after filtration, with the feed concentrations known from solution preparation and the filtrate concentrations correlated from absorbance values.

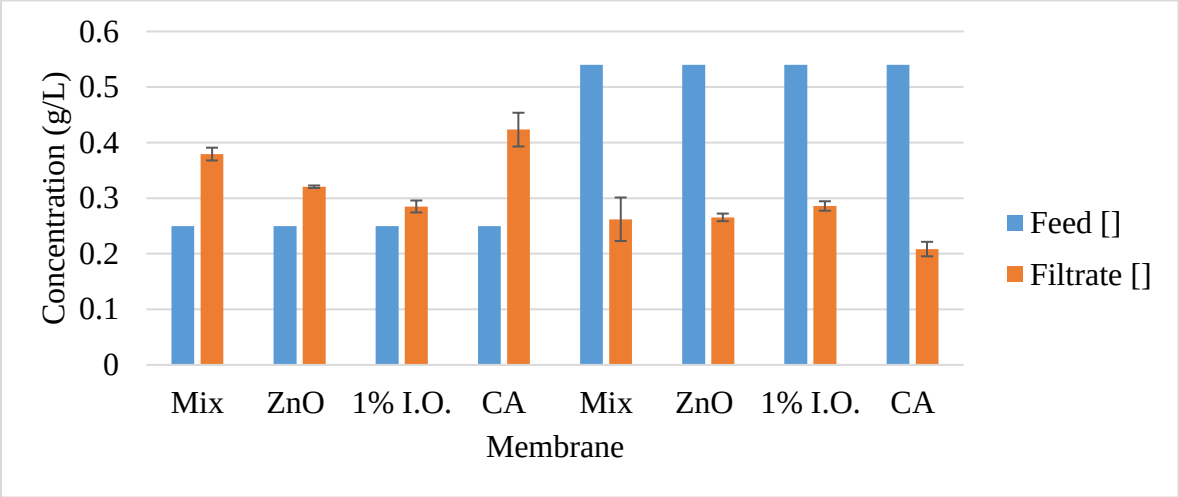

Figure 4.8 Copper (II) concentrations before and after filtration through various membranes

The error bars presented in the figure above relates to the variation in absorbance measurements and converted to concentration by the relation described in the calibration curve. The calibration does not seem to be accurate in estimating concentration however, because the filtrates from runs with a feed concentration of 0.25 g/L were calculated as higher than the feed. These results show that the lower end of the calibration curve was likely overestimating concentration levels, so feed concentrations in further tests were kept at 0.6 g/L. While the results cannot be considered significant, Figure 4.8 shows a generally lower filtrate concentration at higher feed load rates. This

could possibly be related to the solution pH and its effects on membrane surface charge. As a 0.6 g/L solution had a measured pH of around 3.8, lowering copper salt concentrations would trend towards neutral. Figure 4.9 investigated the rejection of copper by the membranes with a feed concentration of 0.6 g/L and a pH of 8.5.

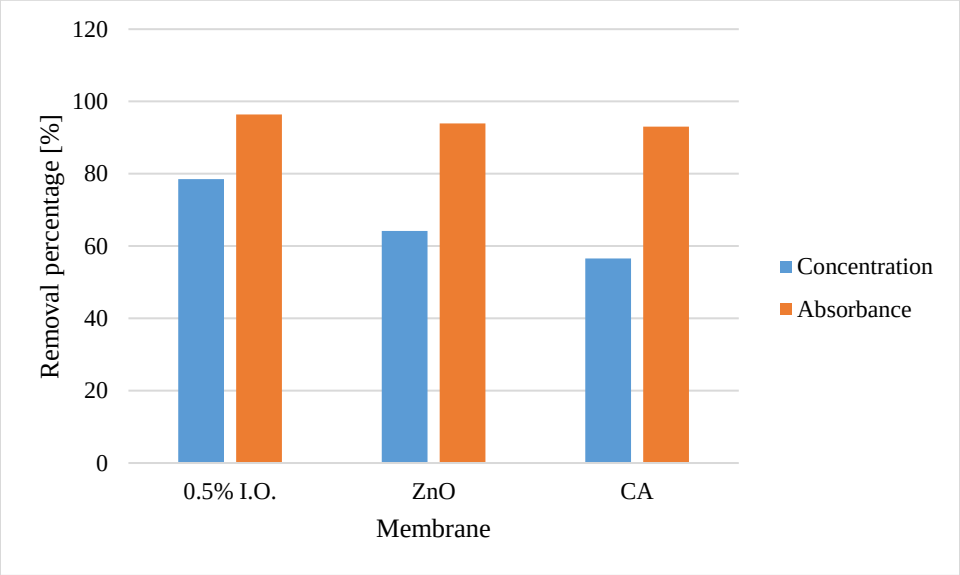

Figure 4.9 Removal rates by different membranes of Cu(II) from 0.6 g/L feed solution at a pH of 8.5 by concentration calculations and absorbance data

Figure 4.9 shows the removal rates both in terms of directly comparing absorbance values and comparing calculated filtrate concentrations compared to the known feed solutions. As seen above, the removal rates using absorbance levels shows all membranes to have effectively removed over 90% of the copper at a pH of 8.5, with no significant differences seen between membrane types due to the low accuracy of the spectrophotometer. The results using the calibration curve vary significantly from the absorbance calculations, showing removal rates from 57 to 79%, once again bringing the accuracy of the measurement process into question. It should be noted that a higher pH, the Cu(II) ions formed a blue precipitate ($Cu(OH)_2$) [68] and so it is likely that direct comparison of absorbance values is more accurate for estimating the filtration capabilities of the membranes because the calibration curve relates to ions in solution. While there is little information on the removal of metal ions, this graph shows that the membranes are successful at reducing the turbidity of the suspensions.

4.2.2.3 Effect of pH

The comparison of the figures in the section above shows higher removal rates by the membranes at a higher pH, likely due to the precipitation of the ions from solution. Figure 4.10 shows the investigation of the removal rates at more incremental pH levels.

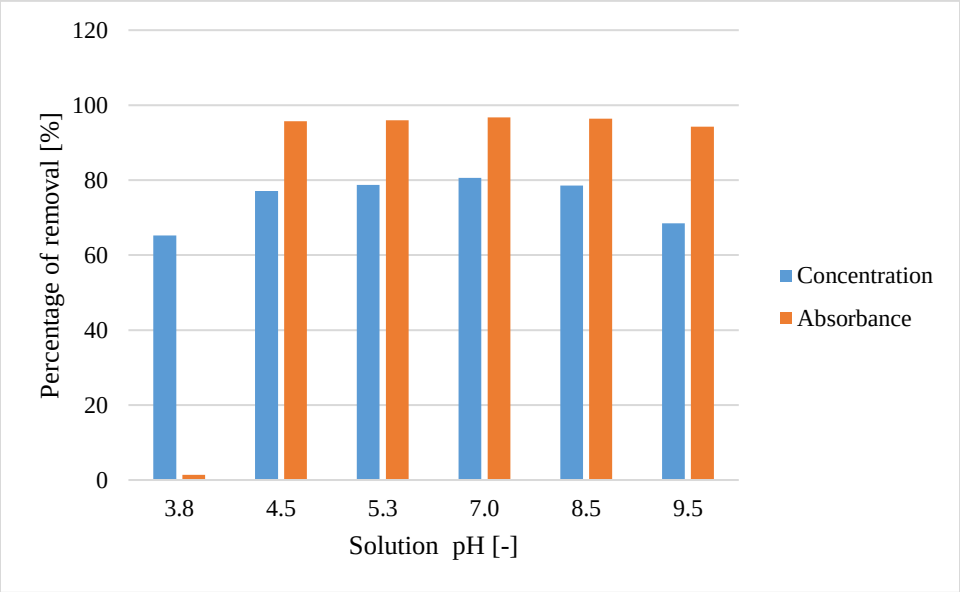

Figure 4.10 Removal rates by 0.5% I.O. membrane of Cu(II) from 0.6 g/L feed solution by concentration calculations and absorbance data at varying solution pH

Figure 4.10 shows the removal of 0.6 g/L of copper in water by 0.5% I.O. membranes at pH levels above 4 to be 94% or higher when comparing direct adsorption values. The results which related outlet absorbance to concentration showed lower removal rates than comparing absorbance levels directly. Neither method showed a significant difference between copper removal at pH levels above 4. All but the 3.8 pH sample had copper precipitates in water instead of copper ions, so the removal mechanism was likely size exclusion of particulates, and the size exclusion mechanism was not shown to be affected by pH levels. The lowest pH level shown (3.8) was the original pH of the copper salt solution, with no precipitation caused by the added base. In comparing the absorbance values of the feed and filtrate, effectively no copper ions were removed by solution. The results by the calibration curve showed near 70% ion rejection, however based on previous findings, this result is likely inaccurate. The inability for the membranes to reject Cu(II) ions could be a factor of the low pH or the high feed concentration, especially considering that metal ion

rejection was successfully observed with arsenic solutions (see Table 3.3) at neutral pH levels and feed concentrations in the scale of tens of μg/L.

4.2.2.4 Ion Adsorption

Finally, the Cu(II) ion adsorption capabilities of the membranes were observed to allow for comparison to filtration results and are presented in Figure 4.11.

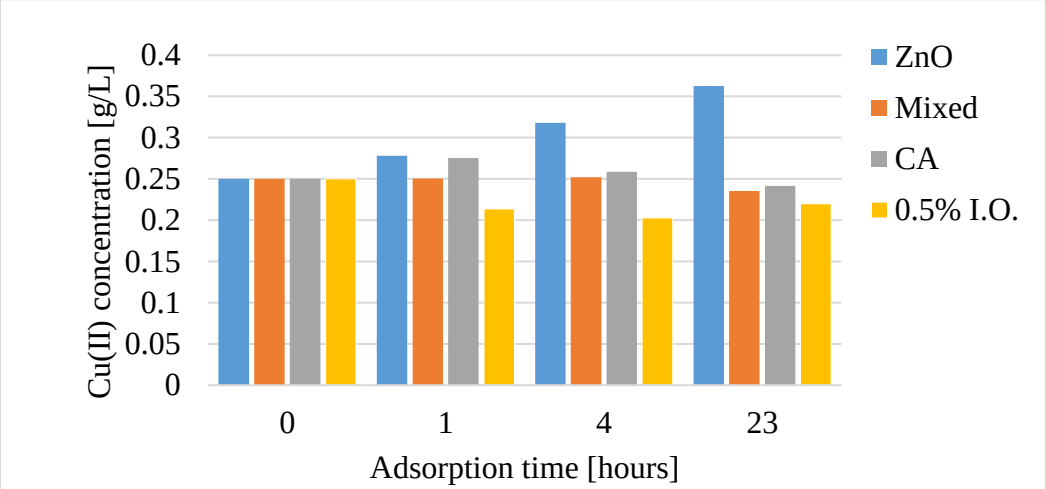

Figure 4.11 Copper (II) concentration in solution with increasing adsorption times

As shown in Figure 4.11, the tested membranes are incapable of removing Cu(II) ions from solution by adsorption as well. Likely due to the fact that the low pH of the solution causes the metal oxides surfaces to have positively charged surfaces, this removes the main adsorption driving force for the system as the Cu(II) ions were positively charged and unable to have electrostatic attraction to the membranes. In contrast to the arsenic adsorption test (Figure 3.9), which successfully adsorbed 60% of arsenic from solution over 24 hours, the Cu(II) ion concentrations weren't observed to decline over a 23 hour period. Once again, the scale of the metal ion concentration may have had an impact. Should some of the metal oxides particles be found to have had negatively charged surfaces, all the available sites could have been occupied by copper ions without a noticeable reduction in concentration in the g/L scale as the number of available adsorption sites was not quantified.

4.3 Microplastics filtration

4.3.1 LDPE particle production

Microplastics filtration was tested using low density polyethylene (LDPE) as well as PS particles whose results were presented in Chapter 3. The methodology for testing was the same as for PS (see section 3.3.3.2). The LDPE microplastics were successfully produced by blending and the particle size distribution of these particles is shown in Figure 4.12.

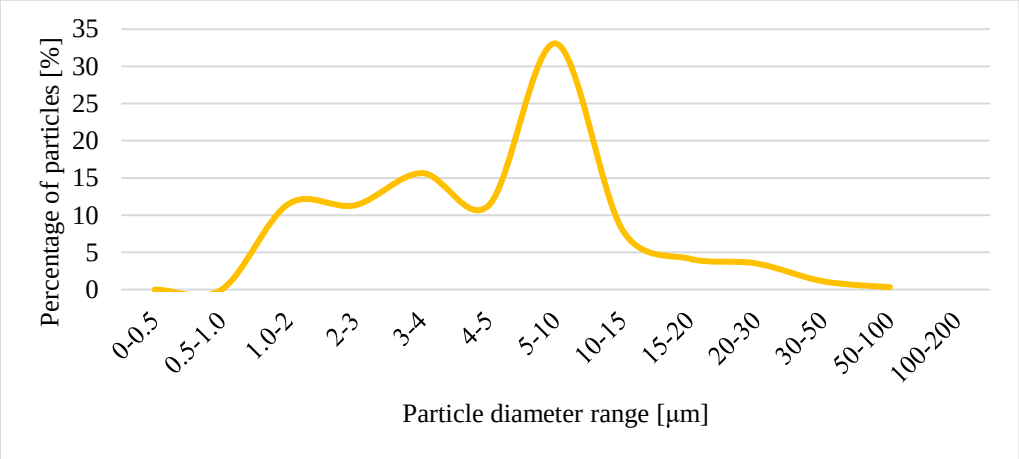

Figure 4.12 Microplastic feed particle size distribution of LDPE feed

Figure 4.12 shows that LDPE particles were produced with sizes from less than 0.5 µm to 1 mm. The LDPE film produced particles with a very similar size distribution to those produced using PS (see Figure 3.10). While the particle sizes were very similar the particle shapes of LDPE particles (see Figure 4.13) were produced from a film and were more like flakes than the straight-edged particles created in PS production (Figure 3.11).

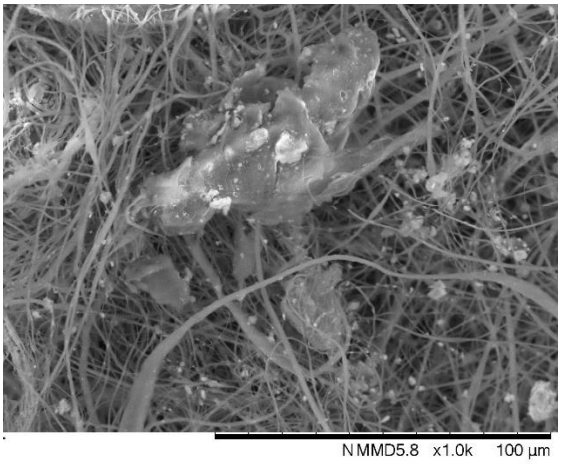

Figure 4.13 Trapped LDPE plastic particles on 2.5% I.O. membrane

4.3.2 LDPE film filtration

Figure 4.14 shows the LDPE size distribution of the filtrates after membrane filtration.

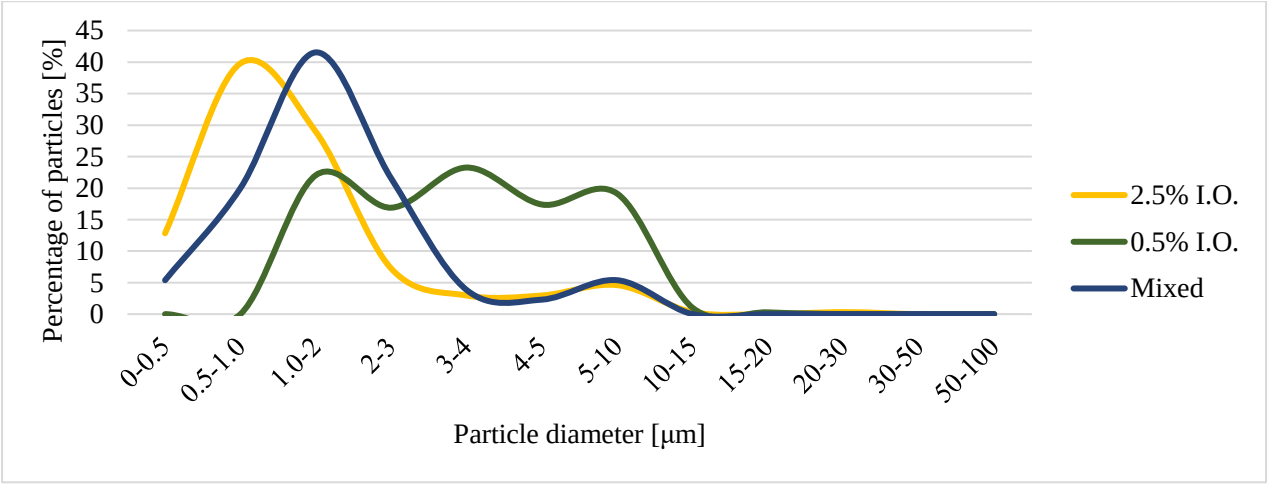

Figure 4.14 Particle size distribution of LDPE filtrates after filtration by various membranes

This graph shows that most particles above 10 µm in size were effectively removed by all membranes. The 0.5% I.O. membrane showed the least success in removing particles above 4 µm in diameter compared to the other tested filters. This is possibly the result of localized a defect in the membrane used for LDPE filtration testing, leading to a higher abundance of pores with slightly larger effective diameters. However, as only one run was tested for each case the significance of the varied filtrate size distribution is negligible. Looking back at the filtrate compositions after filtering PS (see Figure 3.10), the results with LDPE particles are comparable, with all membranes

effectively removing near 100% of particles above 10 µm and showing reduced relative concentrations of particles above 4 µm compared to the feed mixtures. Table 4.2 shows the comparison of the feed and filtrate compositions for LDPE filtration by various membranes by removal percentage.

Table 4.2 Removal rates of LDPE according to particle size

	Particle diameter (µm)						
Membrane	**<2**	**2-5**	**5-10**	**10-15**	**15-20**	**20-50**	**50-100**
0.5 % I.O.	0%	0%	44%	87%	93%	100%	100%
2.5% I.O.	0%	63%	86%	96%	100%	94%	100%
Mixed	0%	21%	84%	100%	100%	100%	100%

Table 4.2 shows the success of rejection of LDPE particles correlates to the observations made from the filtrate distributions. While this quantification method is but an estimate based on normalized size distributions, it allows one to see that the membranes can remove the majority of particles above 10 µm and high amounts of particles (above 80% for 2.5% I.O. and mixed membranes) with sizes from 2 to 5 µm.

The reusability of the membranes when using LDPE as a microplastic material was tested. The filtrate distributions of three filter-rinse cycles are shown in Figure 4.15.

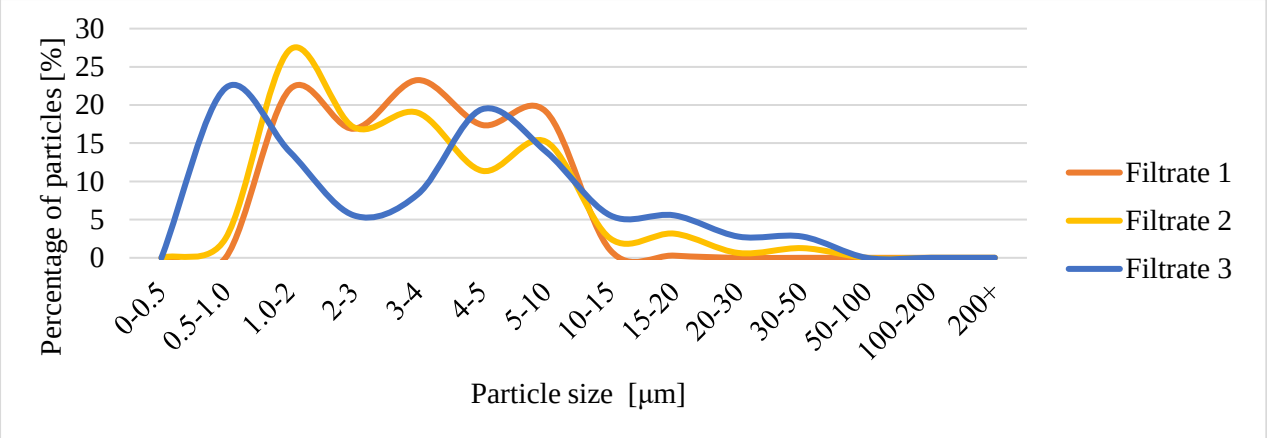

Figure 4.15 Particle size distribution of LDPE particles in filtrates over 3 filtration/rinse cycles using a 0.5% I.O. membrane

Just like what was observed in reusing a neat CA membrane with PS particles (Figure 3.10), Figure 4.15 shows that rinsing increases the lowest particle size effectively removed by the membrane. The comparison of the filtrates to the feed are quantified in Table 4.3.

Table 4.3 Removal rates of LDPE particles after membrane reuse

	Particle diameter (μm)					
Cycle	**<5**	**10-15**	**15-20**	**20-50**	**50-100**	**100+**
Filtrate 1	0%	45%	86%	93%	100%	100%
Filtrate 2	0%	56%	65%	27%	74%	100%
Filtrate 3	0%	60%	23%	0%	23%	100%

The impact of membrane reuse is shown in Table 4.3, where the removal rates of particles above 50 μm drops after each rinse cycle. This suggests that rinsing damages the membranes, even when the particles being removed are more flexible (from a film) than the sharp edged rigid PS.

CHAPTER 5 GENERAL DISCUSSION

Overall these surplus findings show that the membranes made for final testing were successfully optimized given variable spinning conditions. However, longer spinning times caused some defects in the overall membrane mats compared to the sample fibers spun for only 20 minutes. The most impactful variable on fiber morphology was the relative humidity of the system, likely related to the choice of the volatile acetone as the main component of the solvent system.

The produced membranes were not capable of observable copper ion rejection, possibly due to the high concentration of the ions or the low pH caused by the dissolution of the copper salts. The membranes did show some promise at removing turbidity caused by $Cu(OH)_2$ precipitates at higher pH levels, with removal rates above 90% using absorbance as a measurement technique.

Some of the membranes were however capable of ion rejection with arsenic (V) ions, with the best performance by the 2.5% I.O. membrane which gave ~70% of arsenic rejection by direct filtration in standard tap water conditions. The variable success of the membranes for ion removal is likely sue to the effects of pH or of different feed concentrations.

The filtration of LDPE particles from water showed similar results as the filtration tests using PS microplastics. This supports the versatility of the membrane for the removal of various plastic particles, with most effective particle removal being for particle sizes above 10 μm on average. Reusability of the membranes caused reduced performance for both plastic types, likely due to damage of the membranes during the rinsing process. The filtration effectiveness over long term filtration tests using realistic POU MNP pollutant concentrations would be useful to assess the lifespan of the membrane without risking damage of the mats during rinsing.

CHAPTER 6 CONCLUSION AND RECOMMANDATIONS

This work successfully electrospun six membranes made of cellulose acetate with varying compositions of both iron oxide and zinc oxide nanoparticles. The membrane morphologies did not significantly differ from one another in fiber diameter, the average pore sizes of the membranes varied from 2 to 7 µm.

The membranes performance for arsenic removal succeeded in comparison with previous literature. The most successful membrane was the 2.5% iron oxide embedded membrane performing at around 70% arsenic rejection while the cellulose acetate membrane was the second best performing with around 52% arsenic rejection, while the addition of metal oxides at different ratios only worsened rejection performance. Further investigation of the composite membranes with more incremental composition changes can be done to manipulate the surface charge distribution of the membrane and obtain optimal rejection.

The evaluation of heavy metal removal at high concentrations using copper (II) ions proved inconclusive due to the wide range of error in the measurement process by spectrophotometry. However, increasing the solution pH of the copper feed, which caused the copper ions to form oxides, showed that the membranes are capable of removing turbidity from solutions caused by solid particulates. Investigation of higher concentrations of metal ions which do not alter solution pH would be useful to better assess the membranes' behaviours in the future.

These membranes succeeded at removing microplastic particles above around 5 to 10 µm in diameter and could be used for basic ultrafiltration. Metal oxide nanoparticles in the fibers did not have any noticeable impact on micro plastic removal and so plastic filtration can be attributed primarily to membrane morphology.

Some of the sources of errors in these experiments include the uncertainty related to the measurement instruments used. Mainly, the spectrophotometer's error in absorbance measure and loose fitting calibration curve. The resolution of the microscope in microplastic also posed a problem as the presence of larger particles prevented observation of smaller plastics, preventing direct comparison between feed and filtrate mixtures. Unknown contaminants may have also made their way into the various feed solutions in filtration, such as dust, and minor impurities in chemical sources, which may have obscured the findings by interacting with the pollutants or membranes.

The membrane thickness and morphology were also found to vary along the collector length, which could have caused differential properties throughout the final filters.

In conclusion, we can see that in terms of arsenic and microplastic filtration, there is not necessarily a significant reason to include metal oxide nanoparticles in the electrospun membranes as the pure cellulose acetate membrane performed well in both cases. However, further research into the mechanical properties as well as the surface charge of the composite membranes may support their use in water filtration.

Future work in this area could look at more additive concentrations and different additives to improve performance for water filtration. The effects of other pollutants in the water feed on membrane selectivity could be investigated, for example arsenic and microplastics could be filtered together. There are a wide range of other pollutants, such as various heavy metals or organic pollutants which can be found in some point of use filtration sites, which could be tested for filtration by this works filters in order to test their versatility. Finally, it could be useful to look analyse the life cycle of these membranes to compare their economic and environmental cost compared to other water treatment methods.

REFERENCES

[1] H. Yang, S. Xu, D. E. Chitwood, and Y. Wang, "Ceramic water filter for point-of-use water treatment in developing countries: Principles, challenges and opportunities," *Front. Environ. Sci. Eng.*, vol. 14, no. 5, p. 79, May 2020, doi: 10.1007/s11783-020-1254-9.

[2] K. W. Brown, B. Gessesse, L. J. Butler, and D. L. MacIntosh, "Potential Effectiveness of Point-of-Use Filtration to Address Risks to Drinking Water in the United States," *Environ Health Insights*, vol. 11, p. 1178630217746997, Dec. 2017, doi: 10.1177/1178630217746997.

[3] R. M. Blair, S. Waldron, V. Phoenix, and C. Gauchotte-Lindsay, "Micro- and Nanoplastic Pollution of Freshwater and Wastewater Treatment Systems," *Springer Science Reviews*, vol. 5, no. 1, pp. 19–30, Dec. 2017, doi: 10.1007/s40362-017-0044-7.

[4] R. A. Castañeda, S. Avlijas, M. A. Simard, and A. Ricciardi, "Microplastic pollution in St. Lawrence River sediments," *Can. J. Fish. Aquat. Sci.*, vol. 71, no. 12, pp. 1767–1771, Dec. 2014, doi: 10.1139/cjfas-2014-0281.

[5] GRACE Communications Foundation, "Hydraulic Fracturing and its Impact on Water Resources," *Water Footprint Calculator*, Oct. 13, 2018. https://www.watercalculator.org/footprint/fracking-water/ (accessed Nov. 09, 2021).

[6] M. Lapierre, "Lead contamination widespread in Montreal: investigation," *Montreal*, Nov. 04, 2019. https://montreal.ctvnews.ca/lead-contamination-widespread-in-montreal-investigation-1.4669865 (accessed Nov. 12, 2021).

[7] Institut national de sante publique de Quebec, "Arsenic," *INSPQ*, Apr. 27, 2021. https://www.inspq.qc.ca/eau-potable/arsenic (accessed Nov. 12, 2021).

[8] A. A. Koelmans, N. H. Mohamed Nor, E. Hermsen, M. Kooi, S. M. Mintenig, and J. De France, "Microplastics in freshwaters and drinking water: Critical review and assessment of data quality," *Water Res*, vol. 155, pp. 410–422, May 2019, doi: 10.1016/j.watres.2019.02.054.

[9] World Health Organization, "Arsenic," Feb. 15, 2018. https://www.who.int/news-room/fact-sheets/detail/arsenic (accessed Oct. 18, 2021).

[10] H. Garelick, H. Jones, A. Dybowska, and E. Valsami-Jones, "Arsenic pollution sources," *Rev Environ Contam Toxicol*, vol. 197, pp. 17–60, 2008, doi: 10.1007/978-0-387-79284-2_2.

[11] Y. Tian *et al.*, "Electrospun membrane of cellulose acetate for heavy metal ion adsorption in water treatment," *Carbohydrate Polymers*, vol. 83, no. 2, pp. 743–748, Jan. 2011, doi: 10.1016/j.carbpol.2010.08.054.

[12] N. G. Society, "Great Pacific Garbage Patch," *National Geographic Society*, Jul. 05, 2019. http://www.nationalgeographic.org/encyclopedia/great-pacific-garbage-patch/ (accessed Nov. 01, 2021).

[13] L. M. Hernandez, E. G. Xu, H. C. E. Larsson, R. Tahara, V. B. Maisuria, and N. Tufenkji, "Plastic Teabags Release Billions of Microparticles and Nanoparticles into Tea,"

Environmental Science & Technology, vol. 53, no. 21, pp. 12300–12310, Sep. 2019, doi: 10.1021/acs.est.9b02540.

[14] S. Bukhary, J. Batista, and S. Ahmad, "Design Aspects, Energy Consumption Evaluation, and Offset for Drinking Water Treatment Operation," *Water*, vol. 12, no. 6, Art. no. 6, Jun. 2020, doi: 10.3390/w12061772.

[15] R. Liang, A. Hu, M. Hatat, and N. Zhou, "Fundamentals on Adsorption, Membrane Filtration, and Advanced Oxidation Processes for Water Treatment," vol. 22, 2014, pp. 1–45. doi: 10.1007/978-3-319-06578-6_1.

[16] A. W. Mohammad, Y. H. Teow, W. L. Ang, Y. T. Chung, D. L. Oatley-Radcliffe, and N. Hilal, "Nanofiltration membranes review: Recent advances and future prospects," *Desalination*, vol. 356, pp. 226–254, Jan. 2015, doi: 10.1016/j.desal.2014.10.043.

[17] A. Abdelkader, "A REVIEW OF MEMBRANE BIOREACTOR (MBR) TECHNOLOGY AND THEIR APPLICATIONS IN THE WASTEWATER TREATMENT SYSTEMS," Mar. 2007.

[18] K. El Tayara, "Cleaning and characterization of radioactive wastewater with hollow fiber membrane filters," 2013. doi: 10.13140/RG.2.2.21818.59840.

[19] J. Xue, T. Wu, Y. Dai, and Y. Xia, "Electrospinning and Electrospun Nanofibers: Methods, Materials, and Applications," *Chem Rev*, vol. 119, no. 8, pp. 5298–5415, Apr. 2019, doi: 10.1021/acs.chemrev.8b00593.

[20] "(PDF) Electrospinning Jets and Nanofibrous Structures." https://www.researchgate.net/publication/51079287_Electrospinning_Jets_and_Nanofibrous_Structures (accessed Nov. 12, 2021).

[21] L. Persano, A. Camposeo, C. Tekmen, and D. Pisignano, "Industrial Upscaling of Electrospinning and Applications of Polymer Nanofibers: A Review," *Macromolecular Materials and Engineering*, vol. 298, no. 5, pp. 504–520, 2013, doi: 10.1002/mame.201200290.

[22] F. Fadil, N. D. N. Affandi, M. I. Misnon, N. N. Bonnia, A. M. Harun, and M. K. Alam, "Review on Electrospun Nanofiber-Applied Products," *Polymers (Basel)*, vol. 13, no. 13, p. 2087, Jun. 2021, doi: 10.3390/polym13132087.

[23] M. Es-saheb and A. Elzatahry, "Post-Heat Treatment and Mechanical Assessment of Polyvinyl Alcohol Nanofiber Sheet Fabricated by Electrospinning Technique," *International Journal of Polymer Science*, vol. 2014, pp. 1–6, 2014, doi: 10.1155/2014/605938.

[24] L. Wang, C. Shi, L. Wang, L. Pan, X. Zhang, and J.-J. Zou, "Rational design, synthesis, adsorption principles and applications of metal oxide adsorbents: a review," *Nanoscale*, vol. 12, no. 8, pp. 4790–4815, Feb. 2020, doi: 10.1039/C9NR09274A.

[25] C. Potla Durthi, S. B. Rajulapati, A. A. Palliparambi, A. K. Kola, and S. H. Sonawane, "Studies on removal of arsenic using cellulose acetate–zinc oxide nanoparticle mixed matrix membrane," *Int Nano Lett*, vol. 8, no. 3, pp. 201–211, Sep. 2018, doi: 10.1007/s40089-018-0245-3.

[26] H. Cramail, B. Bizet, O. Lamarzelle, P.-L. Durand, G. Hibert, and E. Grau, "Bio-Sourced Polymers: Recent Advances," in *Advanced Green Chemistry Part 2: From Catalysis to Chemistry Frontiers*, vol. 6, I. T. Horváth and M. Malacria, Eds. World Scientific Publishing Company (WSPC), 2020, pp. 167–328. doi: 10.1142/9789811210587_0005.

[27] R. J. R. Matos, C. I. P. Chaparro, J. C. Silva, M. A. Valente, J. P. Borges, and P. I. P. Soares, "Electrospun composite cellulose acetate/iron oxide nanoparticles non-woven membranes for magnetic hyperthermia applications," *Carbohydrate Polymers*, vol. 198, pp. 9–16, Oct. 2018, doi: 10.1016/j.carbpol.2018.06.048.

[28] T. Fan and R. Daniels, "Preparation and Characterization of Electrospun Polylactic Acid (PLA) Fiber Loaded with Birch Bark Triterpene Extract for Wound Dressing," *AAPS PharmSciTech*, vol. 22, no. 6, p. 205, Jul. 2021, doi: 10.1208/s12249-021-02081-z.

[29] K. Shinyama, "Mechanical and Electrical Properties of Polylactic Acid with Aliphatic-Aromatic Polyester," *Journal of Engineering*, vol. 2018, p. e6597183, Jun. 2018, doi: 10.1155/2018/6597183.

[30] C. P. Jiménez-Gómez and J. A. Cecilia, "Chitosan: A Natural Biopolymer with a Wide and Varied Range of Applications," *Molecules*, vol. 25, no. 17, p. 3981, Sep. 2020, doi: 10.3390/molecules25173981.

[31] H. R. Le, S. Qu, R. E. Mackay, and R. Rothwell, "Fabrication and mechanical properties of chitosan composite membrane containing hydroxyapatite particles," *J Adv Ceram*, vol. 1, no. 1, pp. 66–71, Mar. 2012, doi: 10.1007/s40145-012-0007-z.

[32] C. Carrizales *et al.*, "Thermal and mechanical properties of electrospun PMMA, PVC, Nylon 6, and Nylon 6,6," *Polymers for Advanced Technologies*, vol. 19, no. 2, pp. 124–130, 2008, doi: 10.1002/pat.981.

[33] Michael Bloch, "PVC plastic's environmental impact," *Green Living Tips*, Jan. 04, 2010. https://www.greenlivingtips.com/articles/pvc-and-the-environment.html (accessed Nov. 13, 2021).

[34] F. Kawai, "Biodegradation of Polyethers (Polyethylene Glycol, Polypropylene Glycol, Polytetramethylene glycol, and Others)," in *Biopolymers Online*, American Cancer Society, 2005. doi: 10.1002/3527600035.bpol9012.

[35] V. S. Naragund and P. K. Panda, "Electrospinning of cellulose acetate nanofiber membrane using methyl ethyl ketone and N, N-Dimethylacetamide as solvents," *Materials Chemistry and Physics*, vol. 240, p. 122147, Jan. 2020, doi: 10.1016/j.matchemphys.2019.122147.

[36] J. Puls, S. A. Wilson, and D. Hölter, "Degradation of Cellulose Acetate-Based Materials: A Review," *J Polym Environ*, vol. 19, no. 1, pp. 152–165, Mar. 2011, doi: 10.1007/s10924-010-0258-0.

[37] S. Zepnik, S. Kabasci, R. Kopitzky, H.-J. Radusch, and T. Wodke, "Extensional Flow Properties of Externally Plasticized Cellulose Acetate: Influence of Plasticizer Content," *Polymers*, vol. 5, no. 3, pp. 873–889, Jul. 2013, doi: 10.3390/polym5030873.

[38] The Editors of Encyclopedia Britannica, "cellulose acetate," Jul. 22, 2009. https://www.britannica.com/science/cellulose-acetate (accessed Nov. 12, 2021).

[39] D. Araújo, M. C. Castro, A. Figueiredo, M. Vilarinho, and A. Machado, "Green synthesis of cellulose acetate from corncob: Physicochemical properties and assessment of environmental impacts," *Journal of Cleaner Production*, vol. 260, p. 120865, Mar. 2020, doi: 10.1016/j.jclepro.2020.120865.

[40] S. Majumder, M. A. Matin, A. Sharif, and M. T. Arafat, "Understanding solubility, spinnability and electrospinning behaviour of cellulose acetate using different solvent systems," *Bulletin of Materials Science*, vol. 42, no. 171, pp. 1–9, May 2019, doi: https://doi.org/10.1007/s12034-019-1857-6.

[41] H. Abbasi, H. Fahim, and M. Mahboubi, "Fabrication and characterization of composite film based on gelatin and electrospun cellulose acetate fibers incorporating essential oil," *Food Measure*, vol. 15, no. 2, pp. 2108–2118, Apr. 2021, doi: 10.1007/s11694-020-00799-1.

[42] M. Mehdi *et al.*, "Green Synthesis and Incorporation of Sericin Silver Nanoclusters into Electrospun Ultrafine Cellulose Acetate Fibers for Anti-Bacterial Applications," *Polymers*, vol. 13, no. 9, Art. no. 9, Jan. 2021, doi: 10.3390/polym13091411.

[43] I. Santos-Sauceda, M. M. Castillo-Ortega, T. del Castillo-Castro, L. Armenta-Villegas, and R. Ramírez-Bon, "Electrospun cellulose acetate fibers for the photodecolorization of methylene blue solutions under natural sunlight," *Polym. Bull.*, vol. 78, no. 8, pp. 4419–4438, Aug. 2021, doi: 10.1007/s00289-020-03324-y.

[44] Md. M. Ali, N. Pakkang, S. Taira, K. Koda, K. Itoyama, and Y. Uraki, "Direct Electrospinning of Cellulose Acetate onto Polyurethane Sheet and Effect of Its Saponification on Mechanical Properties," *Journal of Wood Chemistry and Technology*, vol. 39, no. 4, pp. 282–295, Jul. 2019, doi: 10.1080/02773813.2019.1590416.

[45] E. Omollo, C. Zhang, J. I. Mwasiagi, and S. Ncube, "Electrospinning cellulose acetate nanofibers and a study of their possible use in high-efficiency filtration," *Journal of Industrial Textiles*, vol. 45, no. 5, pp. 716–729, Jun. 2014, doi: 10.1177/1528083714540696.

[46] N. Angel, L. Guo, F. Yan, H. Wang, and L. Kong, "Effect of processing parameters on the electrospinning of cellulose acetate studied by response surface methodology," *Journal of Agriculture and Food Research*, vol. 2, p. 100015, Dec. 2020, doi: 10.1016/j.jafr.2019.100015.

[47] Z. Zhou, W. Lin, and X.-F. Wu, "Electrospinning ultrathin continuous cellulose acetate fibers for high-flux water filtration," *Colloids and Surfaces A: Physicochemical and Engineering Aspects*, vol. 494, pp. 21–29, Apr. 2016, doi: 10.1016/j.colsurfa.2015.11.074.

[48] Y. Ertas and T. Uyar, "Fabrication of cellulose acetate/polybenzoxazine cross-linked electrospun nanofibrous membrane for water treatment," *Carbohydrate Polymers*, vol. 177, pp. 378–387, Dec. 2017, doi: 10.1016/j.carbpol.2017.08.127.

[49] S. O. Han, J. H. Youk, K. D. Min, Y. O. Kang, and W. H. Park, "Electrospinning of cellulose acetate nanofibers using a mixed solvent of acetic acid/water: Effects of solvent composition on the fiber diameter," *Materials Letters*, vol. 62, no. 4, pp. 759–762, Feb. 2008, doi: 10.1016/j.matlet.2007.06.059.

[50] K. Wang *et al.*, "Electrospinning of silver nanoparticles loaded highly porous cellulose acetate nanofibrous membrane for treatment of dye wastewater," *Appl. Phys. A*, vol. 122, no. 1, p. 40, Jan. 2016, doi: 10.1007/s00339-015-9566-5.

[51] S. Anitha, B. Brabu, D. John Thiruvadigal, C. Gopalakrishnan, and T. S. Natarajan, “Optical, bactericidal and water repellent properties of electrospun nano-composite membranes of cellulose acetate and ZnO,” *Carbohydrate Polymers*, vol. 97, no. 2, pp. 856–863, Sep. 2013, doi: 10.1016/j.carbpol.2013.05.003.

[52] H. S. Hassan, M. F. Elkady, A. A. Farghali, A. M. Salem, and A. I. A. El-Hamid, “Fabrication of novel magnetic zinc oxide cellulose acetate hybrid nano-fiber to be utilized for phenol decontamination,” *Journal of the Taiwan Institute of Chemical Engineers*, vol. 78, pp. 307–316, Sep. 2017, doi: 10.1016/j.jtice.2017.06.021.

[53] C. Tsioptsias, K. G. Sakellariou, I. Tsivintzelis, L. Papadopoulou, and C. Panayiotou, “Preparation and characterization of cellulose acetate–Fe2O3 composite nanofibrous materials,” *Carbohydrate Polymers*, vol. 81, no. 4, pp. 925–930, Jul. 2010, doi: 10.1016/j.carbpol.2010.04.005.

[54] C. Pittarate, T. Yoovidhya, W. Srichumpuang, N. Intasanta, and S. Wongsasulak, “Effects of poly(ethylene oxide) and ZnO nanoparticles on the morphology, tensile and thermal properties of cellulose acetate nanocomposite fibrous film,” *Polym J*, vol. 43, no. 12, pp. 978–986, Dec. 2011, doi: 10.1038/pj.2011.97.

[55] D. Luo, S. Hu, T. Huang, N. Zhang, Y. Lei, and Y. Wang, “Electrospun Cellulose Acetate/Polyethylenimine Porous Fibers toward Highly Efficient Removal of Cr(VI),” *ACS Appl. Polym. Mater.*, p. acsapm.1c00836, Aug. 2021, doi: 10.1021/acsapm.1c00836.

[56] R. Abedini, S. M. Mousavi, and R. Aminzadeh, “A novel cellulose acetate (CA) membrane using TiO2 nanoparticles: Preparation, characterization and permeation study,” *Desalination*, vol. 277, no. 1, pp. 40–45, Aug. 2011, doi: 10.1016/j.desal.2011.03.089.

[57] A. R. P. Pizzichetti, C. Pablos, C. Álvarez-Fernández, K. Reynolds, S. Stanley, and J. Marugán, “Evaluation of membranes performance for microplastic removal in a simple and low-cost filtration system,” *Case Studies in Chemical and Environmental Engineering*, vol. 3, p. 100075, Jun. 2021, doi: 10.1016/j.cscee.2020.100075.

[58] S. Chattopadhyay, T. A. Hatton, and G. C. Rutledge, “Aerosol filtration using electrospun cellulose acetate fibers,” *J Mater Sci*, vol. 51, no. 1, pp. 204–217, Jan. 2016, doi: 10.1007/s10853-015-9286-4.

[59] M. Kumar, A. M. Isloor, T. Somasekhara Rao, A. F. Ismail, R. Farnood, and P. M. G. Nambissan, “Removal of toxic arsenic from aqueous media using polyphenylsulfone/cellulose acetate hollow fiber membranes containing zirconium oxide,” *Chemical Engineering Journal*, vol. 393, p. 124367, Aug. 2020, doi: 10.1016/j.cej.2020.124367.

[60] M. Kumar, A. M. Isloor, S. R. Todeti, H. S. Nagaraja, A. F. Ismail, and R. Susanti, “Effect of binary zinc-magnesium oxides on polyphenylsulfone/cellulose acetate derivatives hollow fiber membranes for the decontamination of arsenic from drinking water,” *Chemical Engineering Journal*, vol. 405, p. 126809, Feb. 2021, doi: 10.1016/j.cej.2020.126809.

[61] E. Manning, “How to Filter & Remove Microplastics from Tap Water?,” *USA Water Quality*, Aug. 29, 2021. https://www.usawaterquality.org/remove-microplastics-from-tap-water/ (accessed Nov. 16, 2021).

[62] Aaron Stickley, “Materials Used in Water Supply Pipes,” *The Spruce*, Aug. 08, 2021. https://www.thespruce.com/types-of-pipe-used-for-water-2718736 (accessed Nov. 16, 2021).

[63] S. J. Eichhorn and W. W. Sampson, “Statistical geometry of pores and statistics of porous nanofibrous assemblies,” *J R Soc Interface*, vol. 2, no. 4, pp. 309–318, Sep. 2005, doi: 10.1098/rsif.2005.0039.

[64] World Health Organization, “Hardness in Drinking-water.” World Health Organization, 2011. Accessed: Nov. 15, 2021. [Online]. Available: https://www.who.int/water_sanitation_health/dwq/chemicals/hardness.pdf

[65] K. Nakamura, T. Suda, and K. Matsumoto, “Characterization of pore size distribution of non-woven fibrous filter by inscribed sphere within 3D filter model,” *Separation and Purification Technology*, vol. 197, pp. 289–294, May 2018, doi: 10.1016/j.seppur.2018.01.012.

[66] MilliporeSigma, “Water for pH Measurement - Impact of Water,” *Millipore Sigma*, 2021. https://www.emdmillipore.com/CA/en/water-purification/learning-centers/applications/inorganic-analysis/ph-measurement/water-impact/MK6b.qB.3g4AAAFUNWISsxU6,nav?ReferrerURL=https%3A%2F%2Fwww.ecosia.org%2F&bd=1 (accessed Nov. 15, 2021).

[67] J. Pelipenko, J. Kristl, B. Janković, S. Baumgartner, and P. Kocbek, “The impact of relative humidity during electrospinning on the morphology and mechanical properties of nanofibers,” *International Journal of Pharmaceutics*, vol. 456, no. 1, pp. 125–134, Nov. 2013, doi: 10.1016/j.ijpharm.2013.07.078.

[68] Naoto Takeno, “Atlas of Eh-pH diagrams.” National Institute of Advanced Industrial Science and Technology, May 2005. Accessed: Dec. 31, 2021. [Online]. Available: https://www.eosremediation.com/download/Chemistry/Chemical%20Properties/Eh_pH_Diagrams.pdf

APPENDIX A ARTICLE SUPPORTING INFORMATION

Table S. 1 Electrospinning cellulose acetate literature summary

Work	Solid materials	Solution composition	Average fiber diameter (μm)	Proposed application
Abbasi, et al. 2021 [41]	CA	12 wt% in Acetone (Ac) :Acetic Acid (AA) (1 :2)	15	Component of antibacterial films
Mehdi et al., 2021 [42]	CA	17 wt% in Ac :Dimethyl formamide (DMF) (2:1)	0.3	Antibacterial mats (incorporation of sericin-Ag NPs)
Santos-Sauceda et al., 2021 [43]	CA	11 wt% in 80 Ac:water (80:20)	1.22	Dye decolorization
Ali et al., 2019 [44]	CA	9 wt% in Ac:water (90:10)	1.69	N/A
Omollo et al., 2014 [45]	CA	15 wt% in trifluoroacetic acid	~0.12	High efficiency water filtration -NaCl rejection tested (in between 2 nonwoven polypropylene layers)
Naragund and Panda, 2020 [35]	CA	7-15 w/v% in Methyl ethyl ketone (MEK): N,N-Dimethylacetamide (DMAc) (2:1)	0.08 to 0.24	Membrane for water flux (related properties evaluated)
		11-15 w/v % in MEK:DMAc (1:1)	0.12 to 0.2	
		17-19 % w/v in MEK:DMAc (1:2)	0.12 to 0.16	
Angel et al., 2020 [46]	CA	9 to 15% w/v in acetone	0.4 to 1.3	N/A
Zhou et al., 2016 [47]	CA	12 wt% in DMF:Ac (99 :1)	0.96	High Flux water filtration (MP removal see Table 2.4)
		14 wt% in DMF:Ac (99 :1)	1.30	
		16 wt% in DMF:Ac(99 :1)	1.57	
Majumbder et al., 2019 [40]	CA	17 wt% in Ac :DMAc (2 :1)	0.30	N/A
		19 wt% in Ac :DMAc (2 :1)	0.37	

		17 wt% in Ac	1.0	
		19 wt% in Ac	58	
Ertas and Uyar, 2017 [48]	CA	10% (w/v) in DCM :Methanol (4 :1)	0.62	Water treatment (CA and CA/polybenzoxazine membranes)
		12% (w/v) in DCM :Methanol (4 :1)	0.72	
Han et al., 2008 [49]	CA	17 wt% in AA:water (70:30 to 95:5 (w:w))	~0.2 to 1.3	N/A
Tian et al., 2011 [11]	CA	Ac:DMAc	0.75	Heavy metal adsorption (by PMMA surface modification)
Wang et al., 2016 [50]	CA	Ac:AA (2:1)	2.0	Dye adsorption (silver NP additive)
		Ac:DCM (2:1)	4.6	
		Ac:DCM (1:2)	4.9	
Anitha et al., 2013 [51]	CA	14 wt% in DMF:Ac (4:1)	0.17	Bactericidal, optical, and hydrophobic property investigation
Hassan et al., 2017 [52]	CA	Ac:DMF-varying ratios	0.06-0.15	Phenol decontamination
		Ac:DMAc (2:1)	0.06	
		Ac:DMAc (2:1)	0.15	
	CA-ZnO	2:1 Ac:DMAc	~0.6	
Tsioptsias et al., 2010 [53]	CA	20 wt% in Ac:DMAc (2:1)	~0.6	N/A
	CA-Fe2O3		~0.4 (1.4 wt% Fe2O3) ~0.3 (4.5wt% Fe2O3)	
Matos et al., 2018 [27]	CA	12 wt% in Ac:DMAc (2:1 (w:w))	0.299	Magnetic hyperthermia (by Fe3O4 NPs adsorbed onto or embedded in fibers)
	CA	12 wt% in 63:32:5 Ac:DMAc:water	0.272	
	CA-Oleic Acid stabilized Fe3O4 NPs	11 wt% in 63:32:5 Ac:DMAc:water	0.165	
	CA-DMSA stabilized Fe3O4 NPs	10 wt% in 63:32:5 Ac:DMAc:water	0.161	

Figure S. 1 Image of polystyrene particles in water

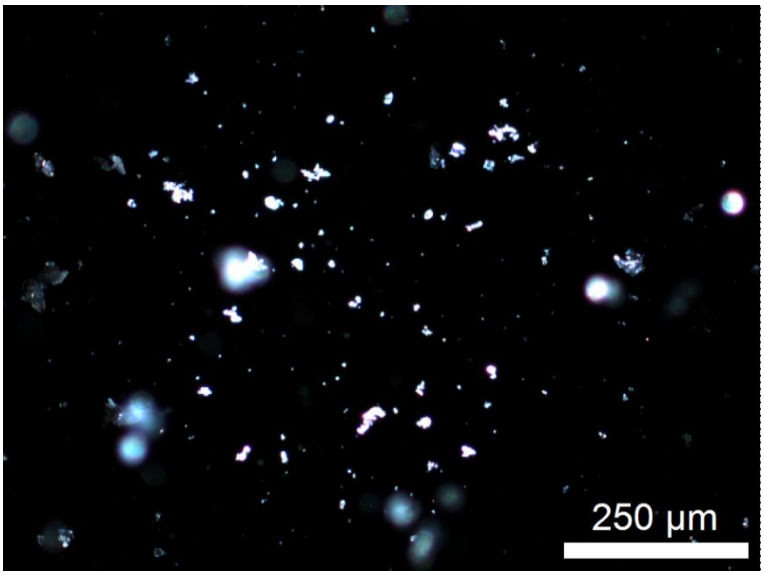

Figure S. 2 Microscopy image of PS particles in water – feed

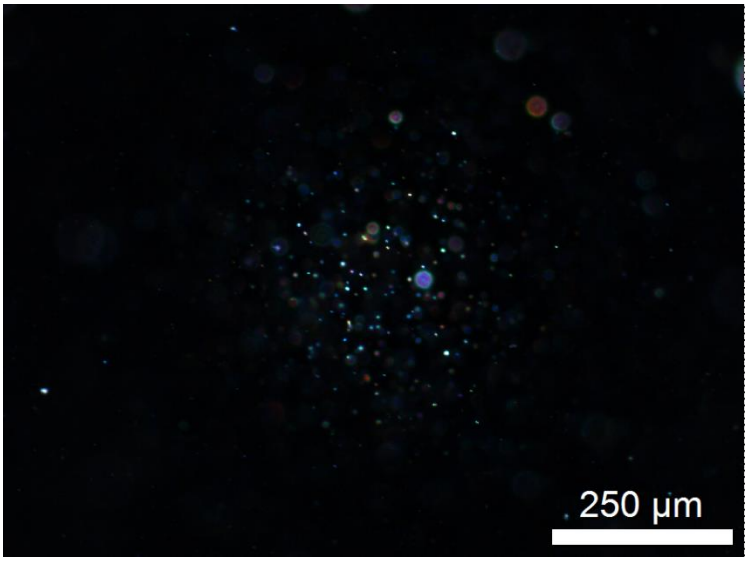

Figure S. 3 Microscopy image of PS particles in water- filtrate after filtration with neat CA membrane